AD-A141 483 APPLICATION OF THE FINITE COMPARTMENT MODEL OF CARBON ADSORPTION TO BINARY SYSTEMS(U) RRMV MILITARY PERSONNEL CENTER ALEXANDRIA VA T R NOREEN MAY 84 1/2

UNCLASSIFIED F/G 7/4 NL

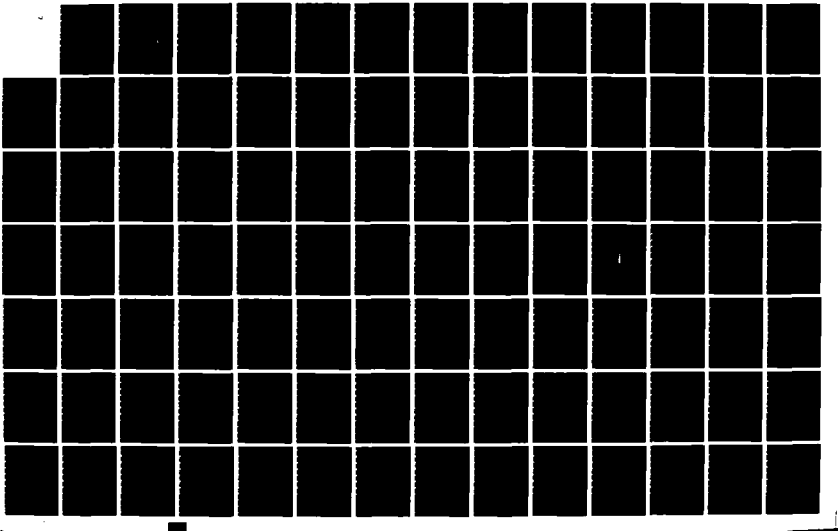

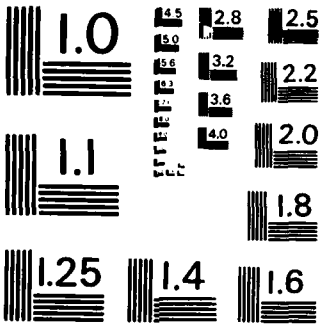

(2)

SECURITY CLASSIFICATION OF THIS PAGE *(When Data Entered)*

REPORT DOCUMENTATION PAGE

READ INSTRUCTIONS BEFORE COMPLETING FORM

1. REPORT NUMBER	2. GOVT ACCESSION NO.	3. RECIPIENT'S CATALOG NUMBER

4. TITLE *(and Subtitle)*
Application of the Finite Compartment Model of Carbon Adsorption to Binary Solute Systems

5. TYPE OF REPORT & PERIOD COVERED
May 1984

6. PERFORMING ORG. REPORT NUMBER

7. AUTHOR(s)
Thomas R. Noreen

8. CONTRACT OR GRANT NUMBER(s)

9. PERFORMING ORGANIZATION NAME AND ADDRESS
Student, HQDA, MILPERCEN (DAPC-OPA-E), 200 Stoval Street, Alexandria, Virginia 22332

10. PROGRAM ELEMENT, PROJECT, TASK AREA & WORK UNIT NUMBERS

11. CONTROLLING OFFICE NAME AND ADDRESS
HQDA, MILPERCEN, ATTN: DAPC-OPA-E, 200 Stovall Street, Alexandria, Virginia 22332

12. REPORT DATE
May 1984

13. NUMBER OF PAGES
112

14. MONITORING AGENCY NAME & ADDRESS*(if different from Controlling Office)*

15. SECURITY CLASS. *(of this report)*
unclassified

15a. DECLASSIFICATION/DOWNGRADING SCHEDULE

16. DISTRIBUTION STATEMENT *(of this Report)*
Approved for public release; distribution unlimited.

17. DISTRIBUTION STATEMENT *(of the abstract entered in Block 20, if different from Report)*

18. SUPPLEMENTARY NOTES
Thesis prepared to fulfill requirements of Master of Science degree at Vanderbilt University.

19. KEY WORDS *(Continue on reverse side if necessary and identify by block number)*
Carbon Adsorption, Granular Activated Carbon, Packed Bed Adsorption, Chemical Engineering

20. ABSTRACT *(Continue on reverse side if necessary and identify by block number)*
see attached sheet

DD FORM 1 JAN 73 1473 EDITION OF 1 NOV 65 IS OBSOLETE

SECURITY CLASSIFICATION OF THIS PAGE *(When Data Entered)*

APPLICATION OF THE FINITE COMPARTMENT MODEL OF CARBON ADSORPTION TO BINARY SOLUTE SYSTEMS

THOMAS R. NOREEN

Thesis under the direction of Professors John Roth and Kenneth Debelak

Successful treatment of wastewater and potable water supplies requires an accurate method of predicting bed size and service life. The design method used must effectively model multicomponent solute systems. The objective of this research is to apply the n-Finite Compartment Model to the binary system of chloroform and methyl isobutyl ketone using a microcolumn technique.

An additional objective is to determine whether there exists a functional relationship between microcolumn and carbon particle diameters which affects the adsorption process.

The microcolumn technique is a cost effective method of dynamically modeling the adsorption process. Reproducible breakthrough curves are obtained in a few hours using a minimal amount of carbon.

The resulting breakthrough curves are numerically evaluated using the method of moments. A linear relationship, independent of column diameter, is found between the first moment and column length. The dimensionless ratios $\mu_{1,j}/\mu_{1,2}$ and $(\mu_1^2/\mu_2)^{.5}$ are functions of column length and hydraulic loading and are not a function of column diameter.

Characteristics of competitive adsorption are observed when comparing the moments of pure component and binary solutions. Moments are not affected by column diameter.

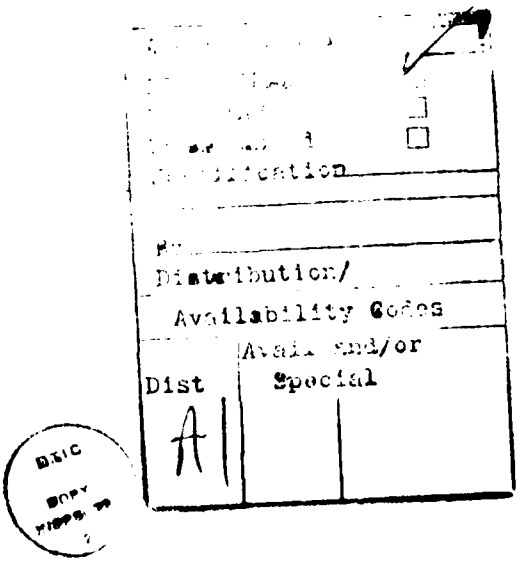

Approval John A. Roth Date April 13, 1984
Advisor

Application of the Finite Compartment Model of Carbon Adsorption to Binary Solute Systems

CPT Thomas R. Noreen
HQDA, MILPERCEN (DAPC-OPA-E)
200 Stovall Street
Alexandria, VA 22332

May, 1984

A thesis submitted to Vanderbilt University, Nashville, TN, in partial fulfillment of the requirements for the degree of Master of Science in Chemical Engineering.

APPLICATION OF THE FINITE COMPARTMENT MODEL OF CARBON ADSORPTION TO BINARY SOLUTE SYSTEMS

By

Thomas R. Noreen

Thesis

Submitted to the Faculty of the

Graduate School of Vanderbilt University

in partial fulfillment of the requirements

for the degree of

MASTER OF SCIENCE

in

Chemical Engineering

May, 1984

Nashville, Tennessee

Approved: John A. Roth — Date: April 13, 1984

Kenneth A. Debelak — Date: April 13, 1984

IN MEMORY OF MY MOTHER

JEAN E. NOREEN

ACKNOWLEDGEMENT

The author is appreciative of the guidance and assistance received from Dr. John A. Roth and Dr. Kenneth A. Debelak during the course of this research. He is also thankful to the U.S. Army for the opportunity to continue his education.

TABLE OF CONTENTS

LIST OF TABLES

LIST OF FIGURES

Figure Page

Figure Page

NOMENCLATURE

A_p	mass transfer area available, cm^2/cm^3
a,b	constants of BDST model
C	liquid concentration, gm/cm^3
D	diameter of microcolumn, inches
F(t)	dimensionless liquid concentration
H	hydraulic loading rate, gal/min-sq ft
K	equilibrium adsorption constant, cm/gm-sec
Kr	rate constant of sorption, min^{-1}
k	mass transfer coefficient, cm/sec
M	equilibrium adsorption constant, gm/cm
N_c	carbon efficiency, gm/cm^3
n	number of CSTR's or FCM's in series
Q	solid concentration, gm/gm
q	liquid flow rate, cm^3/sec
t	time, min
$\bar{t}$	μ_1, mean residence time, min
U	linear velocity of liquid, cm/sec
V	liquid volume in a finite compartment, cm^3
Z	column length, inches
ϵ	bed porosity
μ_i	ith moment, $(min)^i$
ρ_b	bulk density of particle, gm/cm^3

σ μ_2, variance, min^2

ω void of nth compartment/volumetric flow, sec

SUMMARY

Successful treatment of wastewater and potable water supplies requires an accurate method of predicting bed size and service life. The design method used must effectively model multicomponent solute systems. The objective of this research is to apply the n-Finite Compartment Model to the binary system of chloroform and methyl isobutyl ketone using a microcolumn technique.

An additional objective is to determine whether there exists a functional relationship between microcolumn and carbon partical diameters which affects the adsorption process.

The microcolumn technique is a cost effective method of dynamically modeling the adsorption process. Reproducible breakthrough curves are obtained in a few hours using a minimal amount of carbon.

The resulting breakthrough curves are numerically evaluated using the method of moments. A linear relationship, independent of column diameter, is found between the first moment and column length. The dimensionless ratios $\mu_{1,j}/\mu_{1,2}$ and $(\mu_1^2/\mu_2)^{.5}$ are functions of column length and hydraulic loading and are not a function of column diameter. Characteristics of competitive adsorption are observed when comparing the moments of pure component and binary solutions. Moments are not affected by column diameter.

CHAPTER I

INTRODUCTION

History

The first recorded use of carbon for water purification has been found in a Sanskrit manuscript dating from about 200 B.C. This document states: "It is good to keep water in copper vessels, to expose it to sunlight, and filter it through charcoal." (1) Carbon, in the form of bone char, was first commercially used in the late 18th Century for the purification of cane sugar. During the early 19th Century carbon was mainly used as a decolorizing agent. Prior to 1900 a number of municipalities in the United States attempted to use charcoal beds for water purification. These early attempts were later abandoned because ordinary charcoal has relatively poor adsorptive capabilities. The next significant advancement in the use of activated carbon was initiated by the employment of chlorine gas by the Germans in World War I (2). The chemical and food industries have continued to use activated carbon adsorption for the removal of color, odor and other impurities. Since 1970 there has been an increased interest, both in the United States and in Europe, in granular activated carbon (GAC) for the tertiary treatment of wastewater and to improve the quality of drinking water from municipal water systems (3). The concern for tertiary treatment reflects the increased occurrence of hazardous

organics in the nation's water supply. These potentially dangerous substances are found in both influent streams of public water supplies and in the effluents of wastewater treatment systems. In the United States federal and state regulations and public interest have helped to spur the use of GAC systems.

Activated carbon has the unique ability to readily adsorb a wide spectrum of organic compounds effectively and efficiently from aqueous solution. This type of adsorption is representative of isothermal physical adsorption where the adsorbate and adsorbent are weakly bound by van der Waal's forces (4). This is different from chemisorption where the adsorbate becomes chemically bound to the adsorbent. Physical adsorption allows for the cost effective regeneration of the adsorbent. In GAC systems this is done by use of high temperature steam.

Activated carbon's adsorption capability of specific species is a function of the carbon's source material (bone, wood, etc) and how it is produced. As a result one carbon will adsorb a specific compound or family of compounds more effectively than another. To determine the best GAC for a specific application equilibrium isotherm experiments are conducted to calculate the adsorptive capacity of the carbon.

Adsorption Model

The adsorption process of a solute or solutes on activated carbon is a complex, multistep process that has proven difficult to model. Regardless of whether the carbon is in a suspended state (such as an equilibrium shaker bath experiment) or in a fixed bed (packed column),

the same steps occur and the amount of solute adsorbed is greater than can be readily attributed to uptake on the particles surface (5). It has been generally accepted that the physical adsorption process occurs in three steps which can occur in series or in parallel (5):

1. Mass transfer of the solute from the bulk liquid phase to the external surface of the carbon particle (Figure 1).
2. Diffusion of the liquid phase solute from the carbon surface into the macropores of the particle.
3. Micropore diffusion of the solute from the liquid phase into the micropores of the particle.

In packed columns low volumetric flows cause deviation from plug flow and the resulting axial dispersion lowers the adsorption rate. Additionally systems with high solute concentrations in the liquid phase will have mass transfer rates controlled by micropore diffusion of the solute (step 3). In systems, such as wastewater treatment, solute concentrations will be low and mass transfer rates will be controlled by either the mass transfer from the bulk liquid to the solid surface (step 1) or by the macropore diffusion (step 2) from the surface into the particles larger interstitial regions (5).

The current models, as described in the next chapter, assume isothermal operation, linear isotherms, no axial dispersion, and negligible laminar boundary layer resistance. Based on these assumptions the following expressions can be used to describe the various steps of the adsorption model (5,6). The liquid phase transport through the column can be described as:

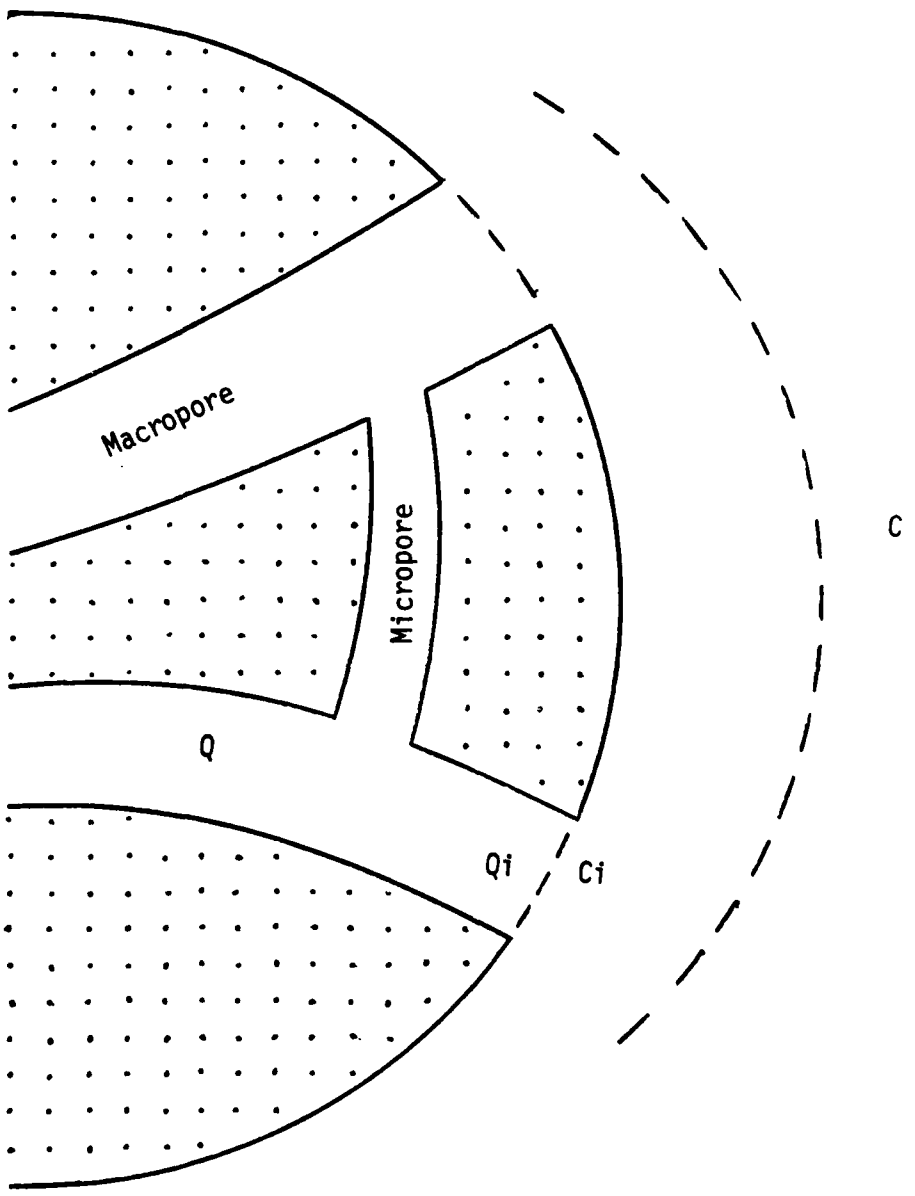

Figure 1. Schematic drawing of adsorption particle pore structure [After Perry et al. (5)].

$$U\frac{\partial C}{\partial z} = \frac{\partial C}{\partial t} + \frac{1-\varepsilon}{\varepsilon}\rho_b \frac{\partial Q}{\partial t} \quad (1)$$

where:

U = linear velocity of the fluid flow, cm/sec.

C = concentration of solute in the liquid phase, gm/cm^3.

ρ_b = bulk density of the carbon, gm/cm^3,

z = column length, cm.

t = time, sec.

ε = bed porosity.

Q = concentration of solute in the solid phase, gm/gm.

The liquid mass transfer rate is defined as (5):

$$\frac{dC}{dt} = k_i A_p (C - C_i) \quad (2)$$

where:

k_i = liquid mass transfer coefficient, cm/sec.

A_p = mass transfer area available, cm^2/cm^3.

C_i = interfacial concentration of the solute, gm/cm^3.

The mass-transfer rate of the solute from the liquid phase to the solid phase can be expressed as:

$$\frac{dQ}{dt} = k_p A_p (Q_i - Q) \quad (3)$$

where:

k_p = solid mass transfer coefficient, cm/sec.

Q_i = interfacial concentration at the surface of the solid, gm/gm.

Isothermal operation permits application of the Freundlich isotherm:

$$Q = KC^n \qquad (4)$$

where:

K = equilibrium adsorption constant.

n = order of adsorption.

The models described in the next chapter endeavor to provide a basis to predict the adsorption process. The models have done this with varying degrees of success depending upon the assumptions made and the complexity of the model used.

Activated Carbon Systems

Fixed bed or packed column granular activated carbon systems are normally operated in one of four configurations. They are either operated in upflow/downflow series or in upflow/downflow parallel (Figure 2). The most efficient and cost effective methods are the series design; however, parallel configurations are used for systems with low solute concentrations and large volume beds.

Series operation obtains the maximum use out of the minimum amount of carbon. In series operation the contaminated stream flows into the leading column where essentially all of the adsorption takes place. As this first column becomes spent, it can no longer adsorb any more solute, and is removed from the system. A replacement column is added at the end of the series. The carbon in the first column can now be regenerated and readied for reuse. In a parallel setup all columns are spent at one time and must be replaced. Depending on the size of the system this

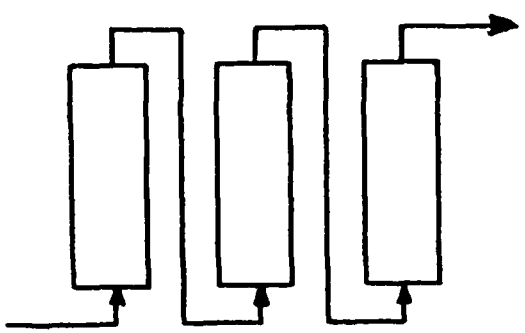

Upflow in series

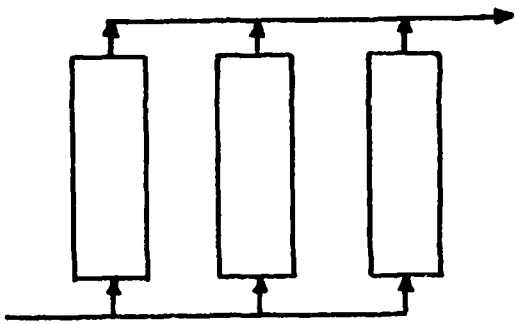

Upflow in parallel

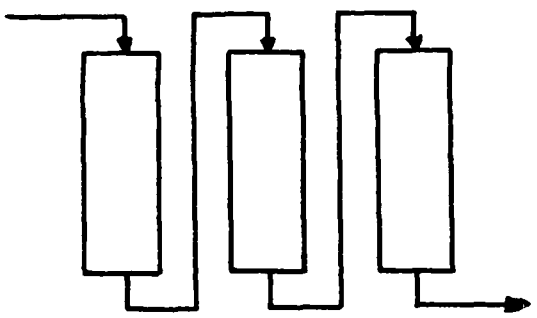

Downflow in series

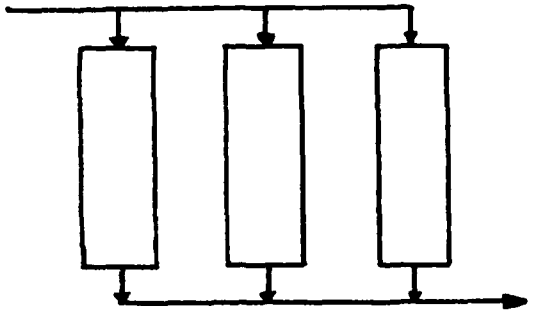

Downflow in parallel

Figure 2. Schematic drawing of activated carbon systems [Nguyen (6)].

could require a considerably larger inventory of carbon. Additionally the parallel system is not as effective at removing the solute. This happens because as the column is used more solute is allowed to pass through even though the column is not considered spent. In a series system the next column is able to adsorb this material that passes through the first column.

CHAPTER II

PRESENT DESIGN METHODS

Like any other unit operation,activated carbon requires an effective and reliable design procedure for efficient and economic operations. Factors of importance in the design of fixed bed or packed columns include the bed depth, service life, and the affinity of the carbon for the specific solute or solutes to be removed. Numerous models have been developed to determine bed depth and service life that vary in complexity and accuracy. Some of these models will be discussed in further detail. To determine the most effective carbon for use with a certain system equilibrium shaker bath experiments provide the most efficient means to screen a large number of different types of carbon. Pilot model studies are often used in conjunction with a proposed design for validation.

The Bed Depth Service Time Model

Bohart and Adams (7) developed the basis for the Bed Depth Service Time (BDST) model while working on the development of military chemical warfare protective masks during World War I. Their studies involved the prediction of the service life for the GAC filters in gas masks when exposed to an atmosphere of chlorine or phosgene gases. This design method was later modified to include more parameters and extended for use in liquid-solid phase systems (8,9). The functional relationship between the thickness of the carbon bed and its useful service life can

expressed as:

$$t = \frac{a\, N_o\, z}{C_o U} - \frac{b}{K C_o} \ln \left(\frac{C_o}{C_b} - 1\right) \qquad (5)$$

where:

t = service time of the adsorbent, sec.

Z = bed depth, cm.

N_o = carbon efficiency, gm/cm^3.

C_o = inlet impurity concentration, gm/cm^3.

C_b = impurity concentration in the effluent at breakthrough, gm/cm^3

U = linear velocity, cm/sec.

K = adsorption constant, $cm^3/gm\text{-}sec$.

a,b = constants for a given system.

The applicability of this equation hinges upon a number of simplifying assumptions (7,10). The first assumption requires that there be no axial dispersion in the adsorber. The next restricts the method to those systems for which the equilibrium isotherm is linear. The third decrees that there exist a proportionality between the adsorption rate, liquid solute concentration and residual carbon capacity. The fourth assumption exacts a functional relationship between diminishing rate of the solute concentration across the bed and the equilibrium isotherm. The final assumption assumes symmetrical S-shaped breakthrough curves.

This method has been widely used because of its simplicity but due to this simplicity its predictive ability varies considerably. Of

the assumptions listed above most frequently it is found that the linear velocity is low enough to allow axial dispersion to take place (11,12) and in many applications the equilibrium isotherms are non-linear (13). Because of these deviations it is necessary to perform pilot scale experiments to validate the proposed BDST design.

The Exchange Zone Model

This method was initially developed by Michaels (14) for predicting the service life of ion exchange resins. The object of Michaels work as described by Treybal (15) shows that for S-shaped break through curves there exists a functional relationship between the height of the adsorptive zone and the constant velocity of the descent of the zone down the adsorber (Figure 3). From this relationship the bed service life can be predicted.

As with the BDST method actual operating conditions are such that axial dispersion usually occurs and many systems exhibit non-linear equilibrium isotherms. The result is that breakthrough curves in general deviate from the classical S-shape and the functional relationship between the adsorption zone height and its velocity down the adsorber are not constant but vary with time.

The shape of the breakthrough curve is influenced by the bed height, particle size, hydraulic loading, and solute concentration. Breakthrough occurs more rapidly with a decrease in bed height and an increase in particle size, hydraulic loading, and solute concentration (15).

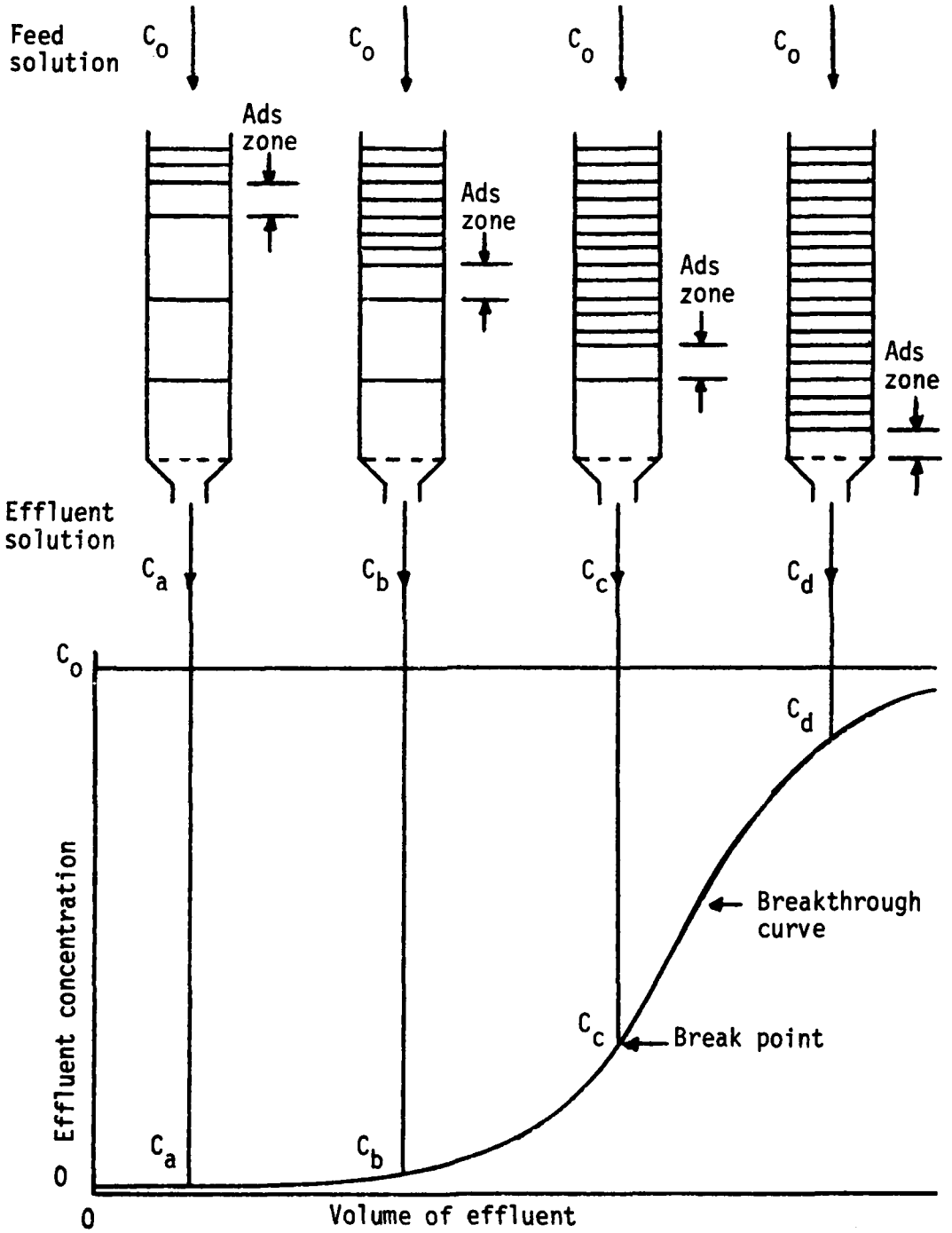

Figure 3. The adsorption wave [Treybal (15)].

n-Continuous Stirred Tank Reactor Model

The n-Continous Stirred Tank Reactors (n-CSTR) in series model as described by Levenspiel (16,17) is a simple one parameter model that accounts for non ideal flow patterns that cause axial dispersion and backmixing.

The concept behind the design method is to consider the liquid phase flow passing through n-equal sized ideal stirred tank reactors. The one parameter that must be solved for in this model is n, the number of ideal stirred tanks. The total volume of the system or its bed size is then the sum of the volumes of the individual tanks.

The material balance for a series of n-CSTR's can be expressed as:

$$QC_{n-1} - QC_n = V \frac{dC_n}{dt} \tag{6}$$

where:

Q = volumetric flow rate, cm^3/sec

C_{n-1} = inlet liquid concentration, gm/cm^3.

C_n = outlet liquid concentration, gm/cm^3.

V = volume of nth tank, cm^3.

t = time, sec.

The response curve representing the change in outlet concentration versus time of nth tank in series can be expressed as (16):

$$F(t) = 1 - \exp[\theta n][1 + n\theta + \frac{(n\theta)^2}{2!} + \cdots + \frac{(n\theta)^{n-1}}{(n-1)!}] \tag{7}$$

where:

$F(t)$ = normalized liquid concentration in nth tank,

n = number of tanks in series,

$\theta = t/\bar{t}$

t = time, min.

$\bar{t}$ = mean residence time, min.

This model has no term accounting for the adsorption or change in concentration of the solute by its adsorption to the carbon particle. Secondly, elements of fluid move at different velocities through the reactor on a molecular scale and the model assumes that all particles have the same mean residence time when determining n, the number of tanks. This deviation may be significantly different from the mean residence time to cause considerable error in determining n. Even with these shortcomings this model often provides satisfactory results in the dynamic modeling of the adsorption process.

n-Finite Compartment Model

The n-Finite Compartment Model (n-FCM) is an extention of the n-CSTR model which includes an adsorption term as a second parameter. This adsorption term takes into account the disappearance of the solutes from the bulk solution. Assuming a first order irreversible reaction for the adsorption of the solute onto the activated carbon a material balance for the solute concentration in the nth finite compartment can be expressed as (4):

$$qC_{n-1} - qC_n = K_r C_n V + V \frac{dC_n}{dt} \qquad (8)$$

where:

q = volumetric liquid flow, $cm^3/min.$

C_{n-1} = inlet liquid concentration, gm/cm^3.

C_n = outlet liquid concentration, gm/cm^3.

K_r = rate constant of adsorption, 1/min.

V = volume of nth finite compartment, cm^3.

t = time, min.

The solution of the response curve as solved by Jenson and Jeffreys (18) for this model is the same as for the n-CSTR model described in Equation 7 with solutions for selected values of n illustrated in Figure 4. The function F(t) can be effectively evaluated from data by using the method of moments (13). Expressions for the first three moments are:

$$\mu_1 = \int_0^\infty (1 - \frac{C_i}{C_o})\, dt \tag{9}$$

$$\mu_2 = \int_0^\infty (1 - \frac{C_i}{C_o}) t_i\, dt \tag{10}$$

$$\mu_3 = \int_0^\infty (1 - \frac{C_i}{C_o})\, t_i^2\, dt \tag{11}$$

Numerical integration of these expressions is readily accomplished through use of numerical integration schemes such as either Simpson's or the trapezoid rule (19).

Haynes and Sarma (6,20) have proposed that the moments of the breakthrough curve are directly related to the physical adsorption

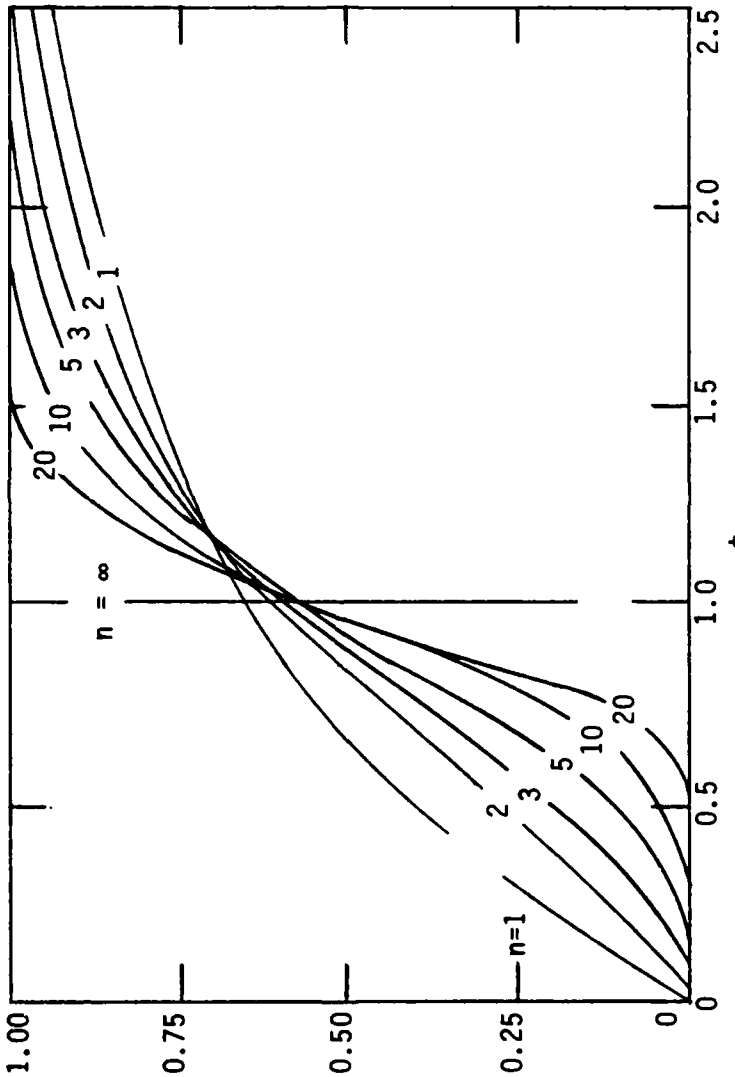

Figure 4. Residence time distribution curves for the n-FCM model [Nguyen (6)].

process. The first moment, or the mean residence time of the adsorber, is related to equilibrium adsorption and is a direct measurement of the amount of solute adsorbed. The second moment, which can also be considered the variance of the system, is associated with intraphase and interphase mass transfer. This includes diffusion of the solute in both solid and liquid phases and accounts for axial dispersion within the column. Evidence to support this is readily discernable when comparing the breakthrough curves of like columns with decreasing hydraulic loads (5). As discussed in the first chapter as the flow rate is diminished axial dispersion increases. Additionally, the slope of the breakthrough curve decreases and the variance increases accordingly (5,17). The physical significance of the third moment is less well understood. The current assumption is that it is an indication of the mass transfer from macropore to micropore or in other words an intraphase transport (6). The mass transfer path of a solute molecule from macropore to micropore decreases in length as a function of time and the rate of this mass transfer also decreases with time. This happens because the number of available adsorption sites decreases and concurrently the rate of diffusion from the micropores to these sites also decreases.

Integration of the first and second moments provides the required information needed to calculate the number of finite compartments. The value of n can be evaluated as (17):

$$1/n = \frac{\mu_2}{\mu_1^2} \qquad (12)$$

where:

μ_1 = first moment or the mean residence time, min.

μ_2 = second moment or the variance, min^2.

The rate constant of adsorption K_r is obtained using the following relationship (4):

$$K_r = \frac{1}{\mu_1} - \frac{q}{V} \tag{13}$$

where:

μ_1 = first moment, min.

q = volumetric flow, cm^3/min.

V = volume of nth finite compartment, cm^3.

The n-FCM model has been further modified (21) to include a third parameter. The material balance for the liquid in the nth compartment can now be written:

$$\frac{d\overline{C}_n}{dt} = \frac{1}{\omega} (\overline{C}_{n-1} - \overline{C}_n) + \frac{K_\rho}{M} (\frac{1-\varepsilon}{\varepsilon}) (\overline{X}_n - \overline{C}_n)$$

where:

ε = bed porosity.

ρ = carbon density, gm/cm^3.

ω = void of nth compartment/volumetric flow rate, min.

K = global mass transfer coefficient, 1/min.

M = equilibrium adsorption constant, gm/cm^3.

X_n = fraction adsorbed in nth compartment.

C_o = initial concentration, gm/cm^3.

C_n = concentration in nth compartment, gm/cm^3.

$\bar{X}_n = MX_n/C_n$.

$\bar{C}_n = C_n/C_o$.

The material balance for the carbon in the nth compartment is:

$$\frac{d\bar{X}_n}{dt} = -K(\bar{X}_n - \bar{C}_n) \qquad (15)$$

Equations 14 and 15 have been solved analytically by Garrison (21) for values of n from 1 to 3.

CHAPTER III

SCOPE OF THIS RESEARCH

The main objective of this research is to experimentally determine whether the n-Finite Compartment Model can be applied to solutions of binary organic solutes using modified high pressure liquid chromatographic (HPLC) equipment as adapted by Nguyen (6) and Rosene (22). Research (6,7,8,10) has been centered on single solute systems. Most water purification designs involve multiple solutes. This will be true for both treatment of wastewater and public water supplies.

The modified HPLC system, which will be described in detail in Chapter IV, allows for the accurate variation of hydraulic loading, bed length, GAC type and particle size, and solute concentration. It is also compact, provides for continuous monitoring, and produces reproducible results in relatively short time intervals of one to four hours depending on hydraulic loading and bed length. The experimental data obtained using this system coupled with the n-Finite Compartment Model provides the necessary information required in the development of a pilot scale study or design of a full scale treatment facility.

Verification of the n-FCM design method using experimental data will be conducted in the following manner:

1. Demonstration of the existence of a relationship between column length and the number of finite compartments within the system.

2. Prediction of experimental breakthrough curves by the model.

The first requirement can be verified by establishing a relationship between the first moment and column length at fixed hydraulic loadings. If this model is to be considered valid then the ratio of the first moments of two columns should equal the ratio of the columns length. Secondly, the ratio of the second moment to the first moment squared should equal one (Equation 12) for any column length and hydraulic loading. Equation 12 should also predict the number of compartments within a system. At a fixed hydraulic loading the ratio of the first moment squared of any column to the second moment of the smallest column should equal the ratio of the column lengths.

The second criteria can be evaluated by calculating the response curve, F(t), as expressed in Equation 7 using experimental data for the unknowns. The resulting curve should be congruent with the actual response curve.

The second objective of this research is to determine whether there exists a relationship between the ratio of column diameter to particle diameter. Critical review of previous studies (6,21) has pointed out that a column diameter to partical diameter ratio of 30 to 1 should be maintained. Even though this fact has been pointed out no evidence has been found in the literature that supports this claim (22-24).

If the column diameter does affect the adsorption process then there should exist differences in the calculated moments. A difference in the first moments calculated for experiments conducted at fixed

hydraulic loadings and column length and variable column diameters would indicate that the amount of solute adsorbed was not the same per unit volume of adsorbent. Different second moments would point to differences in the spread of the response curves obtained and different third moments would demonstrate differences in the general shape or symmetry of these response curves.

CHAPTER IV

EXPERIMENTAL

This chapter presents the experimental plan, experimental procedures followed, data on adsorbent and adsorbates used, and establishes the conditions under which the experiments were conducted.

Adsorbent

Darco HD 4000 activated carbon produced by ICI America, Inc., Wilmington, Delaware, was utilized throughout this research. This carbon was chosen because it readily adsorbed the organic solutes used and was used previously by Nguyen (6). Results from this research could then be directly compared with Nguyen's.

The particle size of the carbon was reduced from a mesh size of 10 by grining with a ceramic mortar and pestle to a mesh of 35 by 60 with a mean particle diameter of 0.01475 inches. The carbon was screened with standard Tyler screens. The retained fraction was rinsed to remove excess fines and any impurities from the carbon surface. It was then autoclaved for a period of eight hours at 120°C to retard any biological growth. The carbon was then stored in air tight flasks until used.

Adsorbates

Chloroform and methyl isobutyl ketone (MIK) were selected as adsorbates for the following reasons:

1. Both are readily adsorbed on activated carbon in sufficient amounts.
2. Both adsorb near-UV light readily and have independent absorption spectra. Chloroform absorbs at 211 nm and MIK at 271.2 nm.
3. Both solutes are found in many wastewater effluents and in the influent water streams to public water supplies and therefore are of environmental concern.

Chloroform and MIK are soluble in water at the concentrations used. The solubility of chloroform at 20°C is 0.82 grams per 100 grams of water and the solubility of MIK is 2.0 grams per 100 grams of water at 20° C (25).

The solutions are prepared as required in one liter amounts on a volumetric basis.

Temperature

The experiments were performed at ambient room temperatures at 20-23° C. This temperature range is within the normal range of temperatures for water and wastewater treatment. No noticeable temperature differences were observed between inlet and outlet streams of the HPLC microcolumn. Shaker bath equilibrium studies were conducted in a water bath maintained at room temperature.

Experimental Plan

The experimental plan was developed to fulfill the objectives of the research and to test the proposed model. The objectives of this

research are to determine whether the n-Finite Compartment Model can be applied to systems of binary solutions and whether a functional relationship exists between the diameter of a column and the diameter of the particles of carbon packing.

The first objective was tested by four sets of experiments. Each set consisted of a series of experiments conducted with fixed column diameter, solute concentration, carbon type and size. Two sets of the experiments were conducted using an ultra violet (UV) monitoring wave length of 211 nm and two were performed at 271.2 nm. At the lower wave length, the spectrophotometer monitors changes in the chloroform concentration and at the upper spectra, changes in the MIK concentration are observed. At each wave length one set of the experiments was run using a binary solution consisting of 300 ppm each of chloroform and MIK in distilled water. The second set at 211 nm was done with a 300 ppm solution of chloroform in distilled water and at 271.2 nm the second set was run with a 300 ppm solution of MIK in distilled water.

Each set of experiments consisted of a series of fifteen runs. Five sets of three runs were conducted at hydraulic loadings ranging from 1.0 to 4.9 gal/min-sq ft. Each of the three runs was done with columns of a different length. The column lengths used were 2, 4, and 6 inches.

The sixty possible sets of data provide the following:

1. Within each of the four sets of data the moments can be compared with columns of equal length at different hydraulic loadings and of different length columns at fixed hydraulic loadings.

2. At each of the UV absorption spectra moments can be compared for columns of the same length at constant hydraulic loadings.

3. Actual response curves can be compared to F(t) curves calculated from Equation 7.

4. Moments of different diameter columns can be compared as a function of hydraulic loading at constant column length.

The first evaluation point is the most important. At a fixed hydraulic loading the ratio of column lengths should equal the ratio of the first moments. Secondly, for any column length, the ratio of the second moment to the first moment squared should equal one. At a constant hydraulic loading the ratio of the first moment squared to the second moment of the shortest column should equal the number of finite compartments and the ratio of column lengths (Equation 7). Evaluation of these points provides the evidence needed to support or refute the validity of this model to the solute or solutes used.

The second point enables a direct comparison of the moments of the binary solute system to that of a single solute. Comparison of the amount of the common solute adsorbed can be accomplished by comparing the first moments for similar data points. This comparison should indicate any trends in competitive adsorption of the different solutes.

The third evaluation point provides a means to test how well the actual data fits the predicted response curve.

Equilibrium shaker bath experiments are performed for each of the pure components and for the binary solution. These are done to evaluate the equilibrium adsorption constant and the linearity of the isotherm.

The second research objective was tested by conducting a single set of experiments during which all variables were held constant except for column diameter and hydraulic loading. Six inch columns with outside diameters of 0.25, 0.375, and 0.50 inches were used. Each of these columns was run at hydraulic loadings ranging from 1.0 to 4.9 gal/min-sq ft.

The fourth evaluation point enables comparison of the moments of each of the three different diameters at constant hydraulic loadings. Equal first moments would indicate that no functional relationship exists between column and particle diameters. A difference in second moments would indicate that the spread or slope of the response curves were different and different third moments would mean the shapes of the response curves were not symmetrical.

Equilibrium Shaker Bath Experiments

Shaker bath batch experiments are performed to determine equilibrium adsorption capacity in grams solute/gram solid. The results of these studies are then fit to the Freundlich isotherm.

The shaker bath experiments were conducted in the following manner. Solutions of MIK, chloroform, and binary mixtures were prepared with concentrations ranging from 100 to 300 ppm with 200 ml of these solutions placed in three 500 ml Erlenmeyer flasks. The GAC was ground to a mesh size of 35 by 60, washed and dried at 120° C. A 2 gram charge of the GAC was then added to each flask and the flask was covered with parafilm.

The flasks were then placed in a Precision Scientific shaker bath.

The water in the shaker bath had previously been equilibrated with the ambient air temperature. The flasks were then agitated for twelve hours. At the end of the twelve hour run, the water phase was decanted and vacuum filtered to remove suspended carbon particles.

Standard solutions were prepared and used to construct a calibration curve for the spectrophotometer. The calibration curve for Chloroform at 211 nm is found in Figure 5 and for MIK at 271.2 nm is found in Figure 6.

Using these calibration curves the filtered water was analyzed using the spectrophotometer to determine the resulting equilibrium concentration. The amount of solute per gram of solid was calculated from a material balance and the isotherms constructed. Sample calculations and the results are found in Appendix A.

Microcolumn Dynamic Experiments

The overall procedure used was developed by Nguyen (6). A diagram of the experimental set up is found in Figure 7. This system consists of a Beckmann Model 110A high pressure liquid chromatograph (HPLC), a Hitachi Model 100-40 Spectrophotometer equipped with an Altex flow cell, a Cole-Parmer Model 252A chart recorder and an Altex six position rotary valve.

The HPLC pump delivers flow rates between 0.0 to 9.9 ml/min in 0.1 ml/min increments using the small capacity pump head. The large capacity pump head operates at volumetric flows of 0.0 to 27.72 ml/min in increments of 0.28 ml/min. Conversions to gal/min-sq ft were calculated to produce hydraulic loads of 1.0, 1.9, 2.8, 3.7 and 4.8 gal/min-sq ft

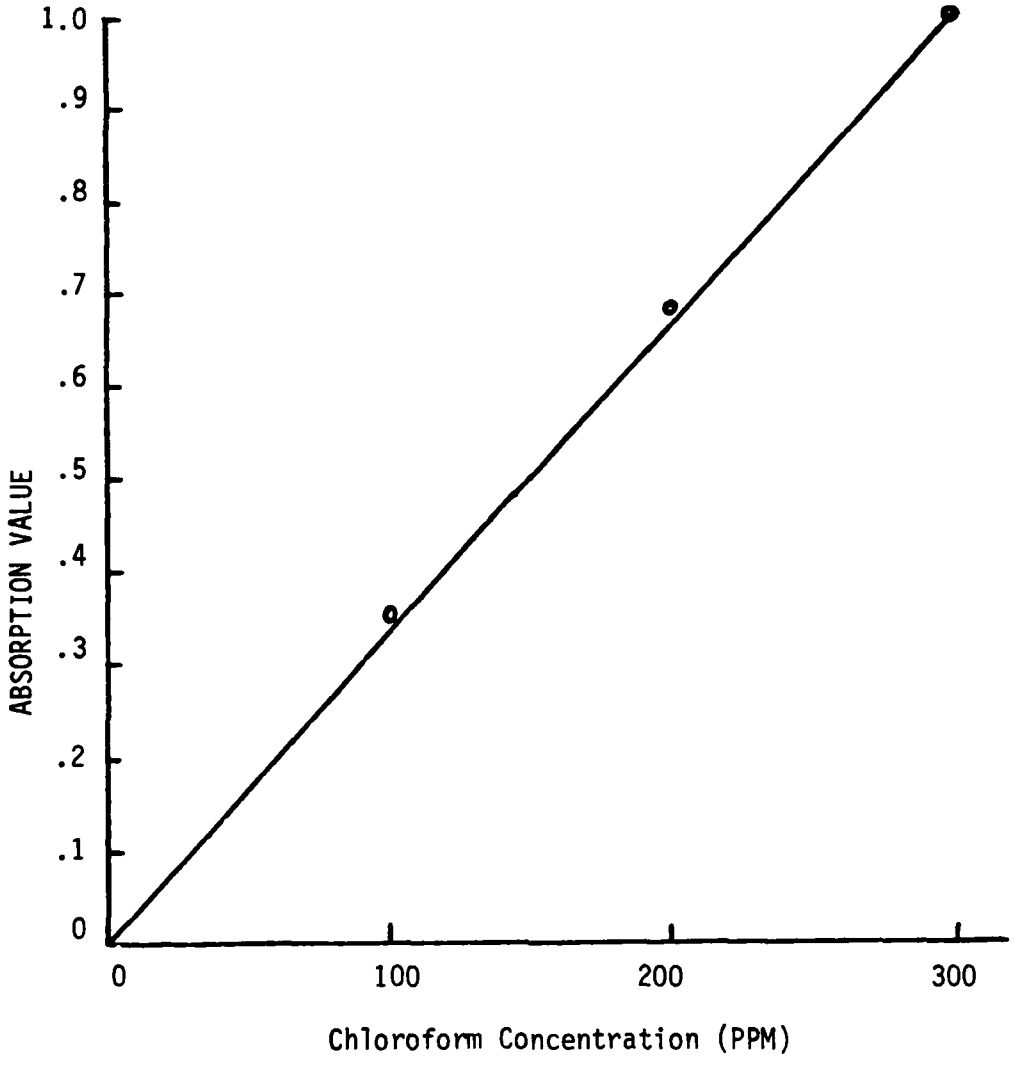

Figure 5. Absorption value of chloroform solutions at UV wavelength of 211 nm.

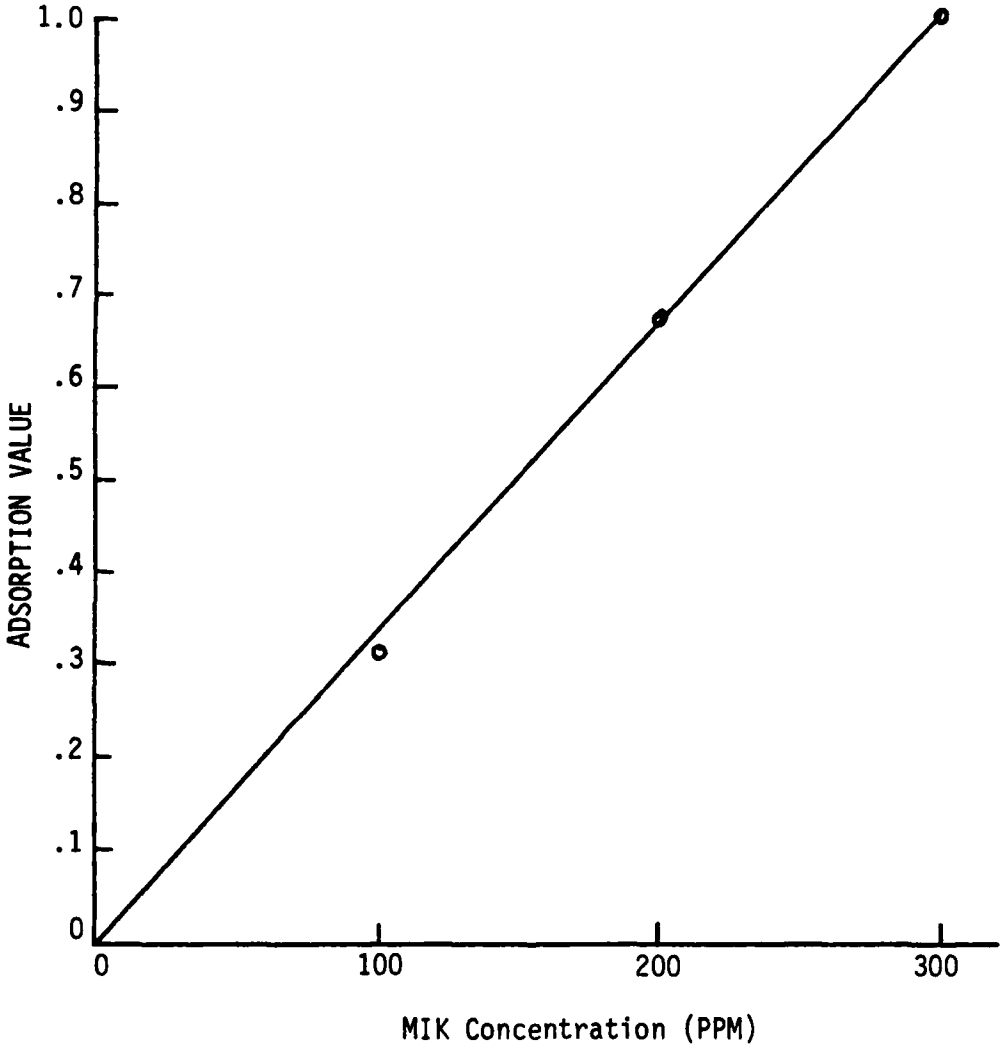

Figure 6. Absorption value of MIK solutions at UV wavelength of 271.2 nm.

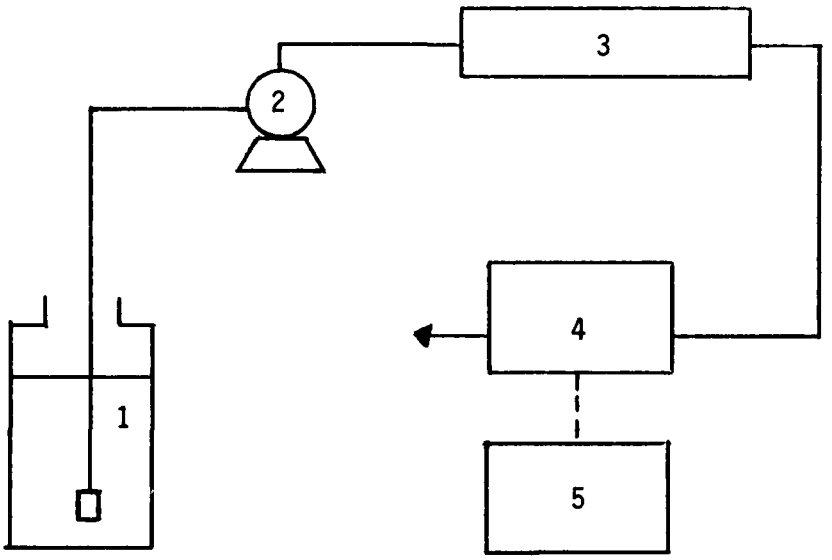

1. Storage tank
2. High pressure pump
3. Microcolumn
4. U-V spectrophometer
5. Chart recorder

Figure 7. Schematic drawing of microcolumn experimental setup [Nguyen (6)].

for each of the three column diameters. These conversions are found in Table 1.

Five microcolumns were used during the course of the research. Columns of 2, 6, and 12 inches length by 0.25 inches OD and columns 6 inches by 0.375 and 0.50 inches OD were used. All columns were made of number 304 stainless steel and had a wall thickness of 0.035 inches. Each of these columns was fitted with Swagelok compression fittings on the ends.

The columns were first weighed empty. The GAC was slowly added and then mechanically settled. The packed column was then weighed. Glass wool was placed in either end to keep the carbon in place and help filter out any fines present. A diagram of a sample packed column is found at Figure 8.

A packed microcolumn was connected to the pump and of the system and flushed with distilled water to remove air from the system and wash out any fines.

The column was then connected to the spectrophotometer and distilled water was pumped through the system to establish the null on the spectrophotometer and the poteniometric recorder.

The experimental run is initiated once the equipment has been zeroed. It is placed into operation by simultaneously switching on the chart recorder and turning the multiposition valve to the correct solution. The system is operated until the spectrophotometer reading reaches and maintains a maximum value. The chart recorder is then stopped and the system flushed with distilled water. A fresh column

TABLE 1

CONVERSIONS OF VOLUMETRIC FLOW
RATE TO HYDRAULIC LOADING

Hydraulic Loading gal/min-sq ft	Column Diameter inches	Volumetric Flow ml/min
1.0	0.25	0.7
	0.375	2.0
	0.50	4.0
1.9	0.25	1.3
	0.375	3.7
	0.50	7.4
2.8	0.25	1.9
	0.375	5.5
	0.50	10.9
3.7	0.25	2.5
	0.375	7.2
	0.50	14.3
4.8	0.25	3.2
	0.375	9.2
	0.50	18.2

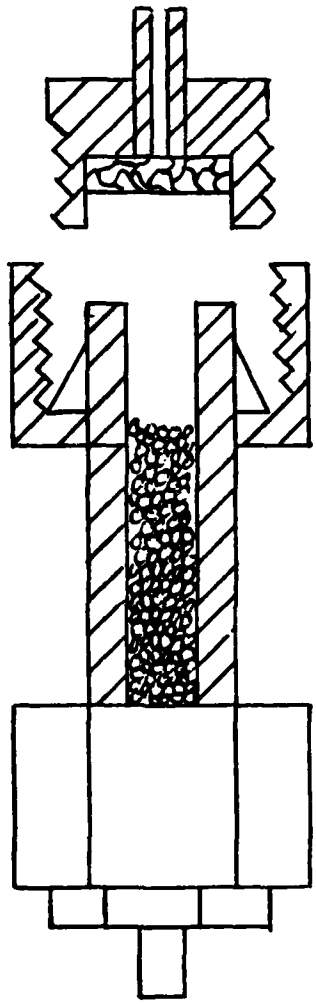

(1) Male swagelok with glasswook inside

(2) Female swagelok with compression fittings

(3) Stainless steel micro-column with activated carbon

Figure 8. Schematic drawing of a packed microcolumn [Nguyen (6)].

is then installed.

The system is calibrated for lag time. This lag is the length of time required for the solution to travel from its container to the flow cell. This calibration is done by inserting a column packed with sand of the same mean particle size as the GAC. The column is then flushed with distilled water and a stop watch is started as the valve is switched to a control solution. The instant the spectrophotometer indicates the presence of the solute the watch is stopped. This is repeated for all column lengths and diameters at each of the hydraulic loadings used. Table 2 contains these results.

TABLE 2

HPLC MICROCOLUMN SYSTEM LAG CONSTANTS

Hydraulic Loadings gal/min-sq ft	Column Diameter inches	Column Length inches	Lag minutes
1.0	0.25	2	11.0
		6	12.1
		12	18.0
	0.375	6	6.0
	0.50	6	3.7
1.9	0.25	2	5.6
		6	7.2
		12	12.0
	0.375	6	3.0
	0.50	6	2.0
2.8	0.25	2	4.0
		6	4.6
		12	7.7
	0.375	6	2.3
	0.50	6	1.2
3.7	0.25	2	3.0
		6	3.5
		12	5.8
	0.375	6	1.7
	0.50	6	1.2
4.8	0.25	2	2.4
		6	2.7
		12	4.6
	0.375	6	1.3
	0.50	6	0.9

CHAPTER V

RESULTS AND DISCUSSION

This chapter presents the results obtained during this research. The method of moments and n-FCM model are discussed. Additionally the results obtained from the column diameter to particle diameter ratio experiments are discussed.

Each breakthrough curve is numerically evaluated using the method of moments. The numerical integration of Equations 9 through 11 is accomplished using the trapezoid rule. A sample calculation of the method of moments is presented in Appendix B along with a copy of the computer program used. The results of these calculations are found in Tables 10 through 15 in Appendix B.

The first moments are plotted against column length as a function of hydraulic loading in Figures 9 through 12. The graphs indicate that the data are linear. As the column length is increased so is the first moment. The first moment represents the mean residence time of the system; therefore, as the size of the system is increased (length of the column) the mean residence time should also increase. Increasing the hydraulic loading decreases the first moment for any particular column length but does not affect the linearity of the moments with regard to column length.

All moments for single solute runs are greater than the corresponding moments of binary solute runs obtained under dynamically similar

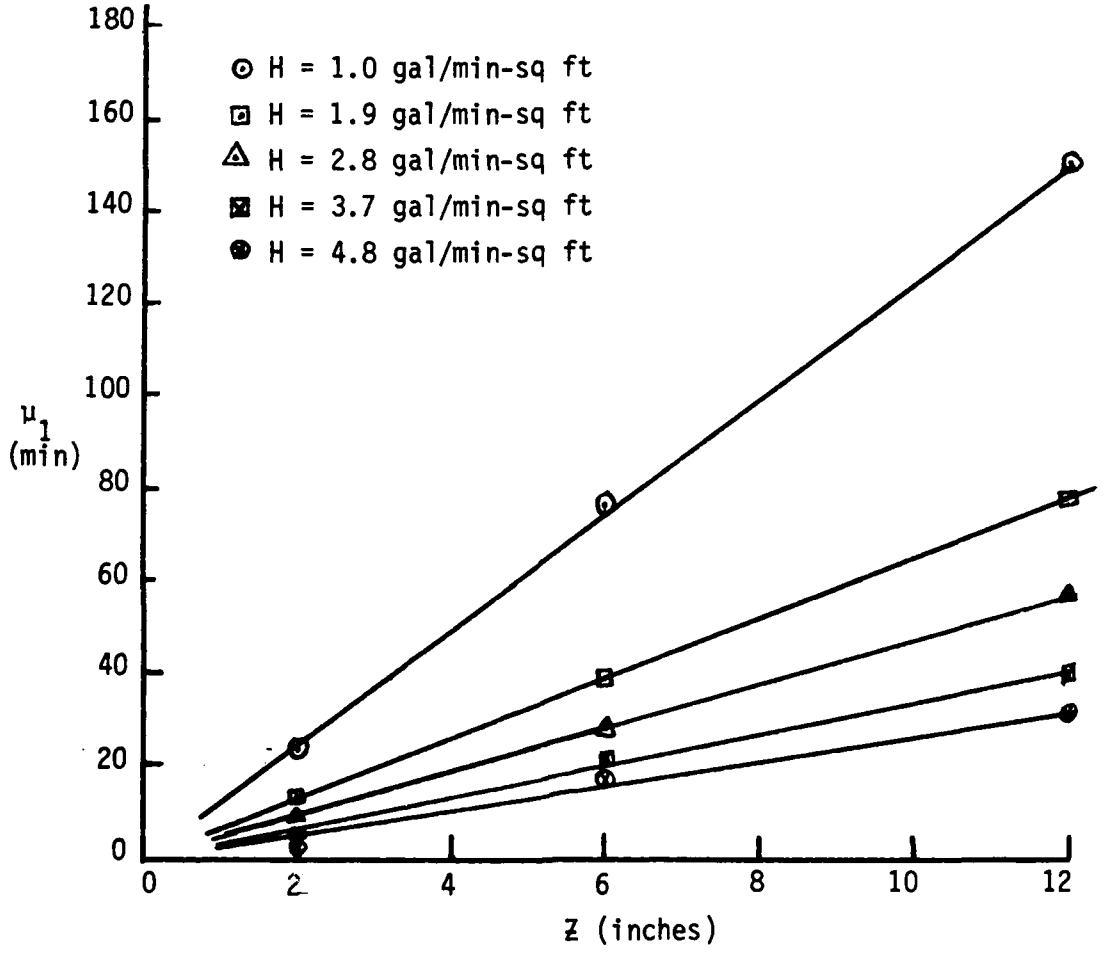

Figure 9. Effect of column length and hydraulic loading on μ_1 for 300 ppm MIK at 271.2 nm.

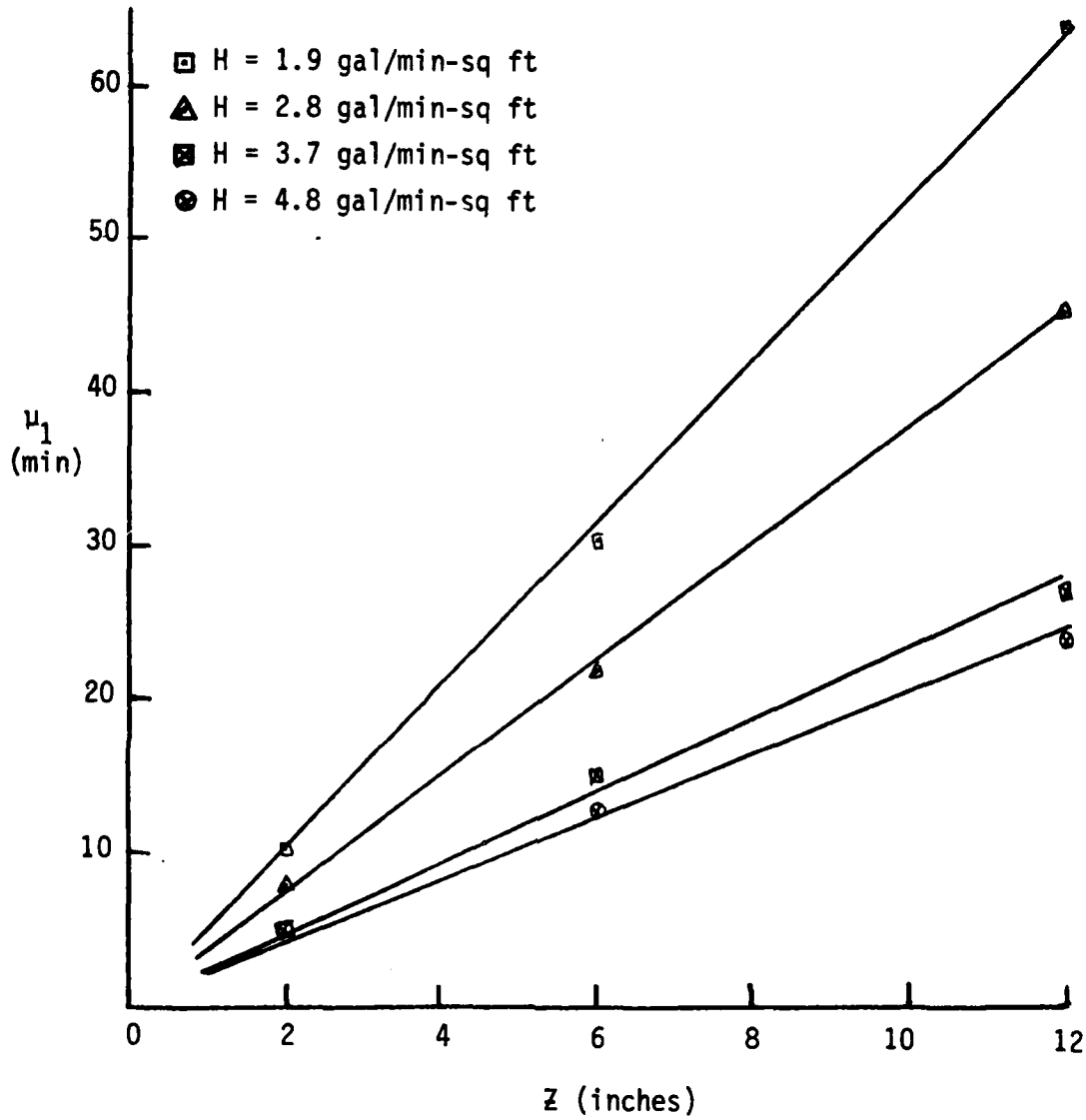

Figure 10. Effect of column length and hydraulic loading on μ_1 for binary solution of 300 ppm MIK and 300 ppm chloroform at 271.2 nm.

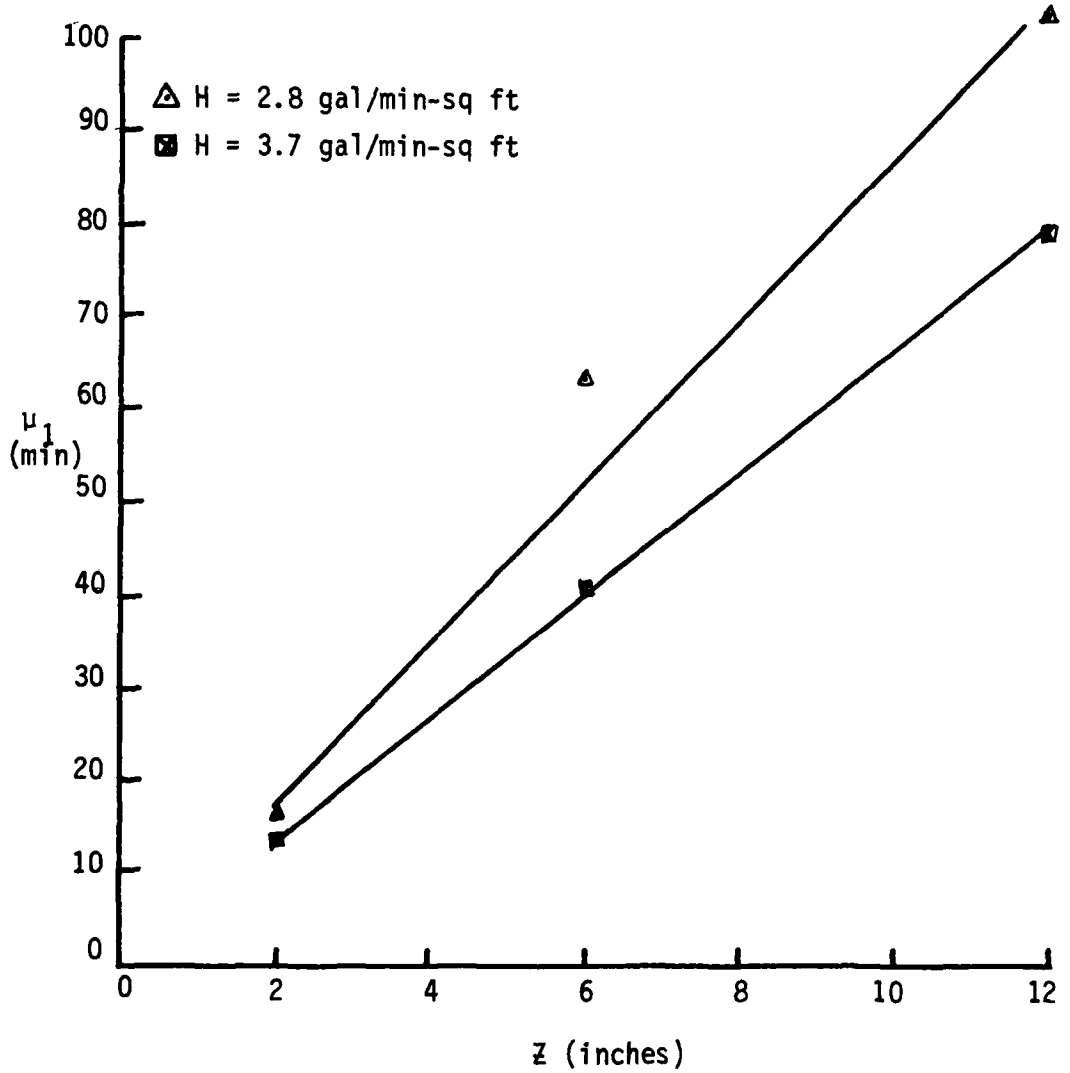

Figure 11. Effect of column length and hydraulic loading on μ_1 for 300 ppm chloroform at 211 nm.

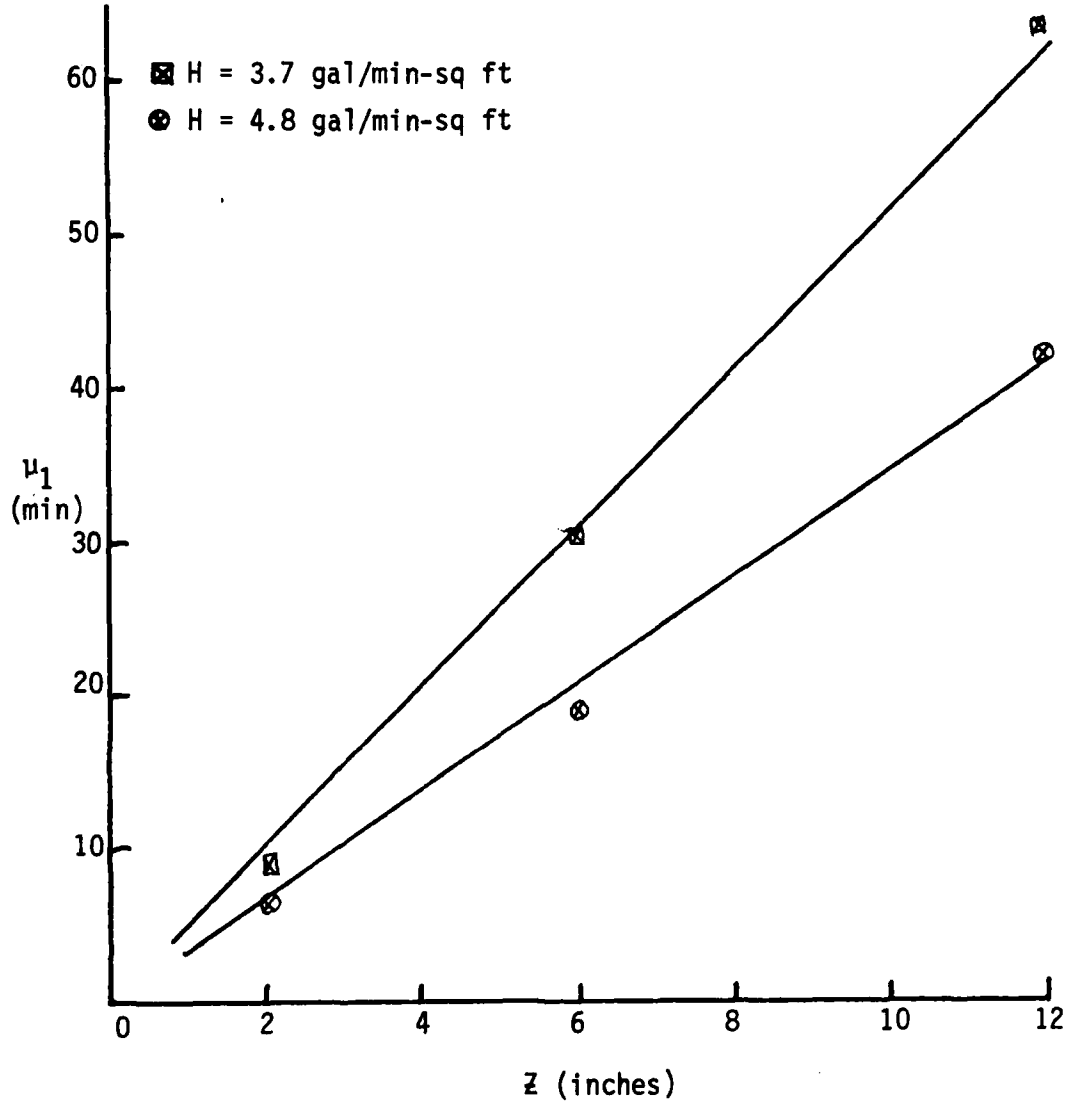

Figure 12. Effect of column length and hydraulic loading on μ_1 for binary solution of 300 ppm chloroform and 300 ppm MIK at 211 nm.

conditions. The ratio of binary moments to single moments is compared for both MIK and chloroform systems. Results of this comparison are found in Tables 3-5. Competition for the available adsorption sites is illustrated by this comparison. Even though the first moment is greater for chloroform than MIK in both single and binary solute runs (see Tables 11-13) the ratio of the first moments of the binary solute to single solute for MIK is consistently larger than its chloroform counterpart (Table 3). This indicates that in the binary solution chloroform adsorption is hindered by the presence of MIK. The result is a binary first moment for MIK that is relatively larger than the binary moment for chloroform when compared to the pure component first moments. There is no doubt that more chloroform is adsorbed. This is supported by the shaker bath experiments and is illustrated in the Fruendlich isotherms presented in Figures 40 and 41 of Appendix A. The point illustrated here is not that more MIK is adsorbed but instead that in a binary solution MIK is more competitive than chlorofrom in occupying the available adsorption sites.

This interference in the adsorption of chloroform can be attributed to the relative size and shape difference between MIK and chloroform. Assuming a spherical shape MIK has an approximate molecular diameter of 74 nm and chloroform has a diameter of about 63 nm (25). Thus MIK is approximately 17 percent larger than chloroform. However MIK is not spherical but relatively linear. The result is that MIK, because of its larger size and greater surface area, tends to block both micropore access and active adsorption sites to the smaller, more compact, chloroform molecule.

TABLE 3

COMPARISON OF FIRST MOMENTS OF
SINGLE SOLUTE SYSTEMS TO
BINARY SOLUTE SYSTEMS

Hydraulic Loading gal/min-sq ft	Column Length inches	$\frac{\mu_1 \text{ Binary}}{\mu_1 \text{ Single}}$ (MIK)	$\frac{\mu_1 \text{ Binary}}{\mu_1 \text{ Single}}$ (chloroform)
4.8	6	0.78	0.62
3.7	12	0.81	0.62
	6	0.74	0.75
	2	0.91	0.58
2.8	6	0.76	0.50
1.0	6	0.81	0.73

TABLE 4

COMPARISON OF SECOND MOMENTS OF
SINGLE SOLUTE SYSTEMS TO
BINARY SOLUTE SYSTEMS

Hydraulic Loading gal/min-sq ft	Column Length inches	$\frac{\mu_2 \text{ Binary}}{\mu_2 \text{ Single}}$ (MIK)	$\frac{\mu_2 \text{ Binary}}{\mu_2 \text{ Single}}$ (choloroform)
4.8	6	0.62	0.43
3.7	12	0.65	0.77
	6	0.57	0.56
	2	0.77	0.49
2.8	6	0.58	0.29
1.0	6	0.65	0.55

TABLE 5

COMPARISON OF THIRD MOMENTS OF
SINGLE SOLUTE SYSTEMS TO
BINARY SOLUTE SYSTEMS

Hydraulic Loading gal/min-sq ft	Column Length inches	$\frac{\mu_2 \text{ Binary}}{\mu_1 \text{ Single}}$ (MIK)	$\frac{\mu_2 \text{ Binary}}{\mu_1 \text{ Single}}$ (chloroform)
4.3	6	0.50	0.31
3.7	12	0.51	0.84
	6	0.44	0.41
	2	0.65	0.34
2.8	6	0.42	0.18
1.0	6	0.53	0.42

The n-FCM model assumes that the total system can be broken down into n equal subsystems. Each finite compartment should then have a first moment that is proportional to n, the number of compartments in the total system. Thus the ratio of first moment of the total system to the individual compartment should equal n. Assuming that n equals one for a two inch column Figures 13 through 16 are plots of the ratio of the first moment of each column length to the first moment of the two inch column. The results indicate that this relationship does exist and that hydraulic loading does not appear to influence this relationship.

The ratio of the first moment squared of any column length to its corresponding second moment should equal one (Equation 12) assuming that each column length is equal to a single finite compartment when compared to itself. Figures 17 through 20 are plots of this ratio versus column length. A straight line can be fitted to this data by least squares. Column length has an effect on this relationship. As the length of the column is increased this ratio approaches one. Possible explanations for this deviation include channelling in the shorter column and the smaller residence times in them. The channelling would cause breakthrough to apparently occur sooner thus, decreasing the residence time. Increased hydraulic loadings can cause channelling and as indicated earlier will decrease the first moment. For dilute solutions the rate controlling step is usually the mass transfer of the solute from the bulk solution to the particle surface. In the shorter columns the convective physical transport of fresh solution

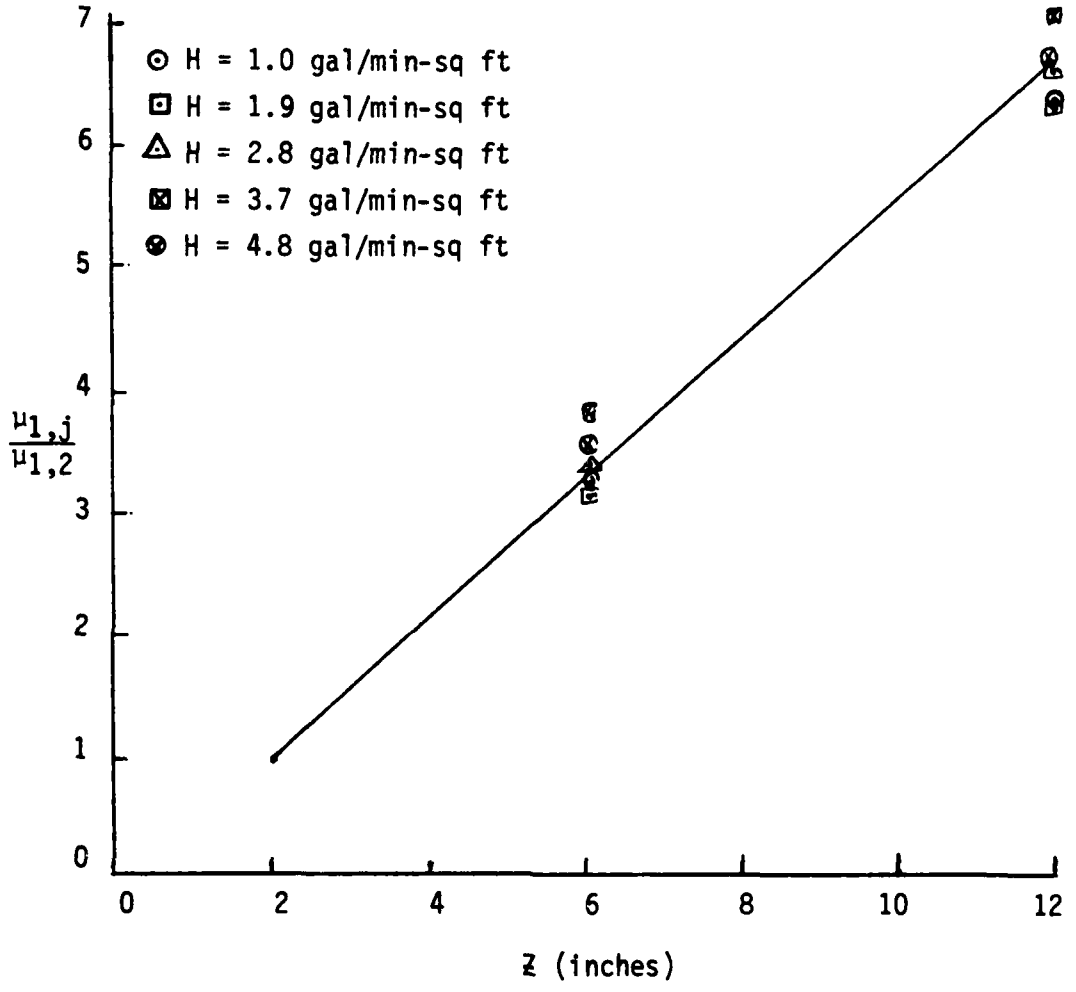

Figure 13. Effect of column length and hydraulic loading on the dimensionless ratio $\mu_{1,j}/\mu_{1,2}$ for 300 ppm MIK at 271.2 nm.

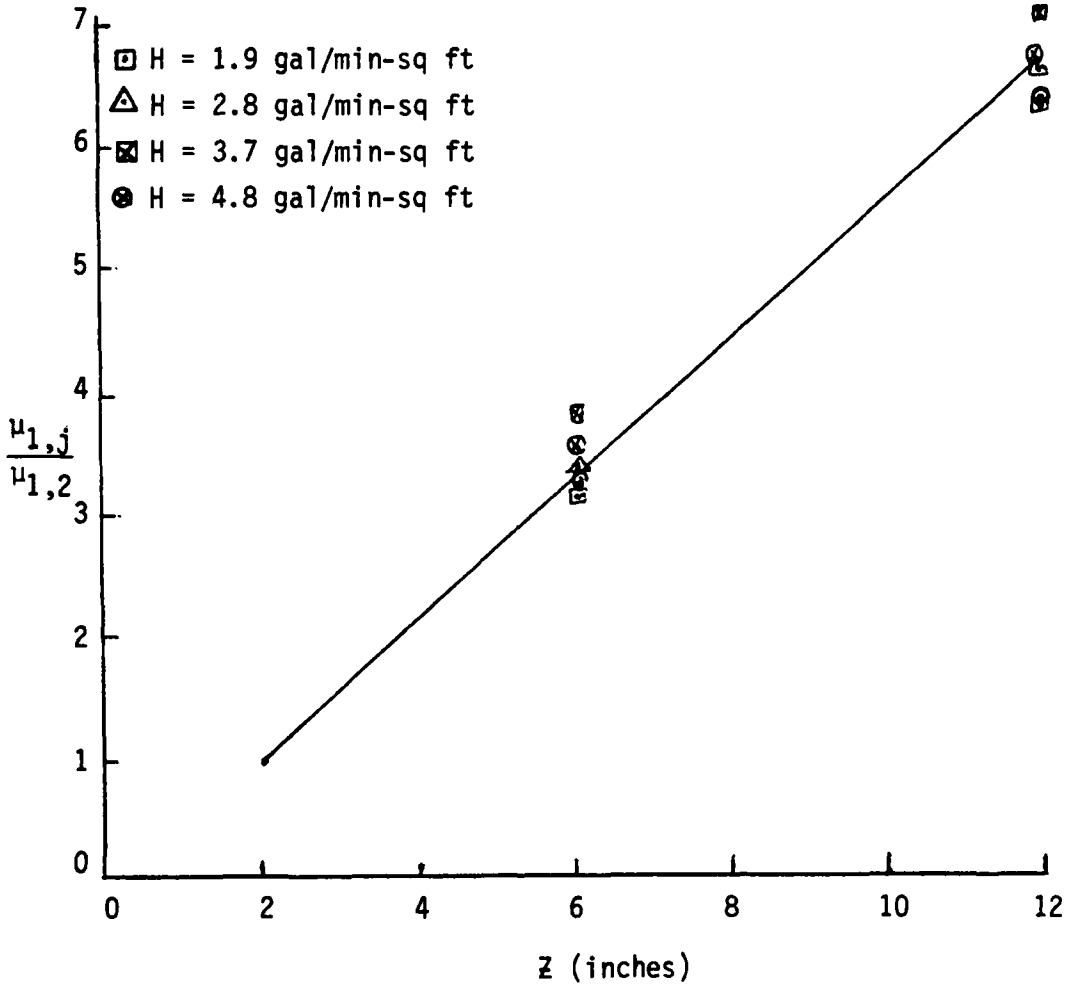

Figure 14. Effect of column length and hydraulic loading on the dimensionless ratio $\mu_{1,j}/\mu_{1,2}$ for binary solution of 300 ppm MIK and 300 ppm chloroform at 271.2 nm.

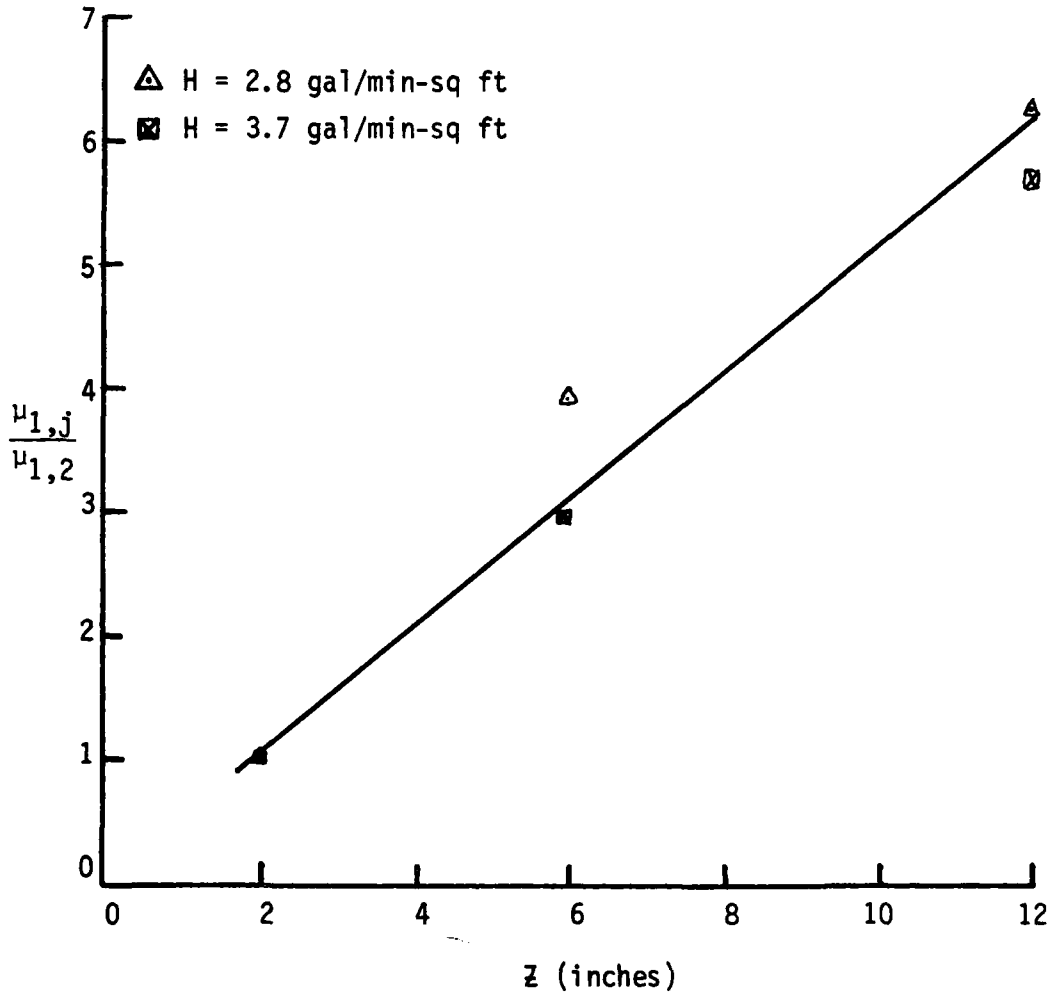

Figure 15. Effect of column length and hydraulic loading on the dimensionless ratio $\mu_{1,j}/\mu_{1,2}$ for 300 ppm chloroform at 211 nm.

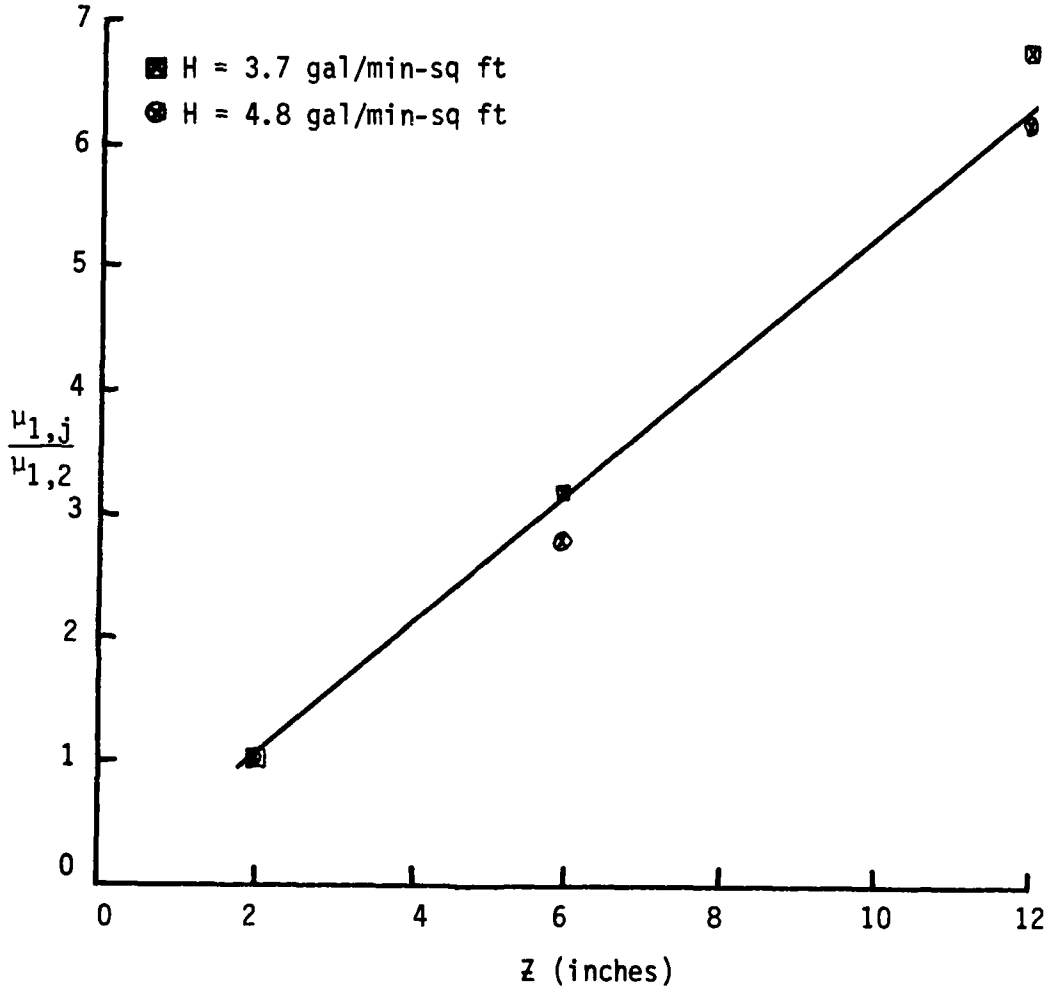

Figure 16. Effect of column length and hydraulic loading on the dimensionless ratio $\mu_{1,j}/\mu_{1,2}$ for binary solution of 300 ppm chloroform and 300 ppm MIK at 211 nm.

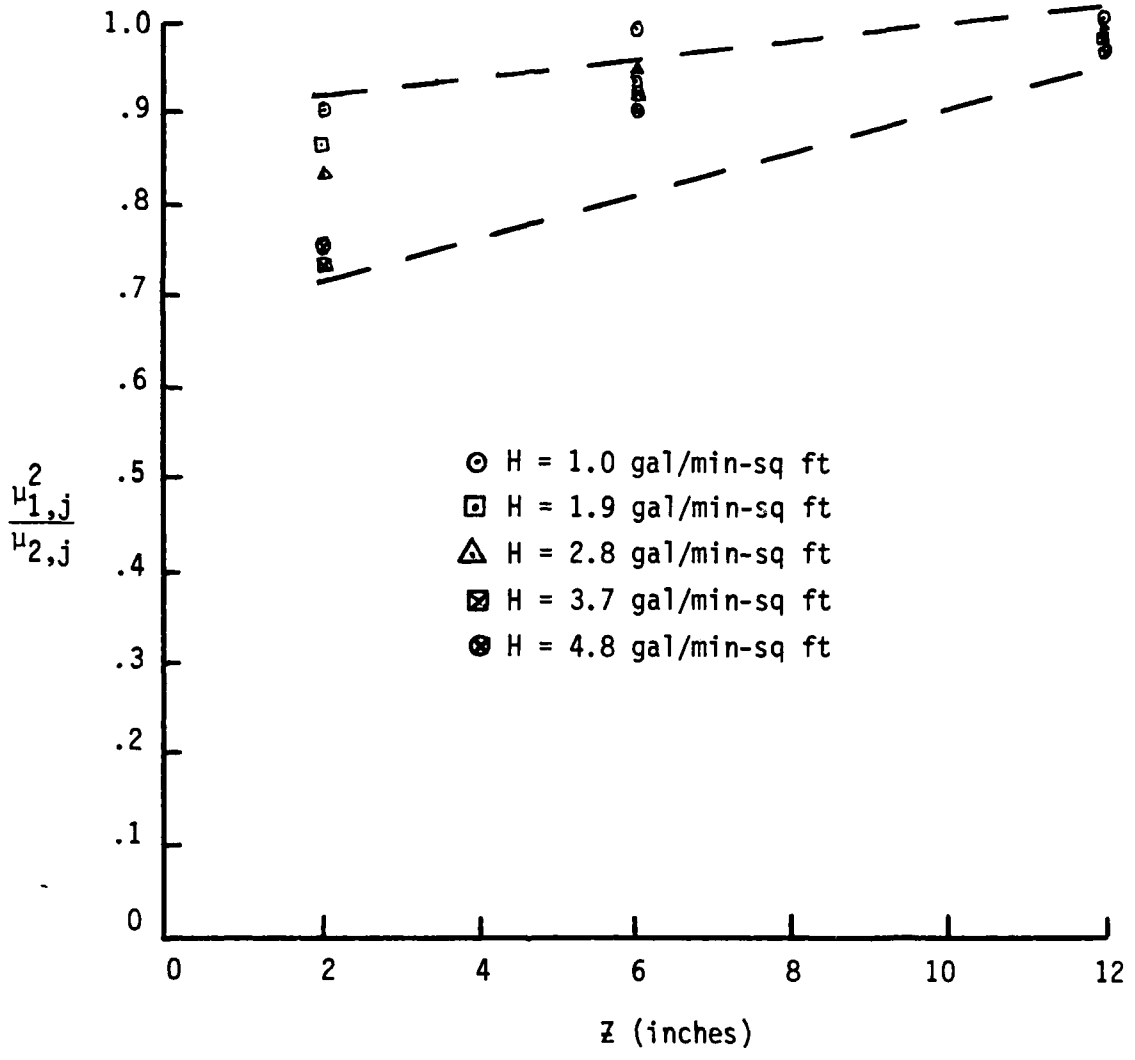

Figure 17. Effect of column length and hydraulic loading on the dimensionless ratio $\mu_{1,j}^2/\mu_{2,j}$ for 300 ppm MIK at 271.2 nm.

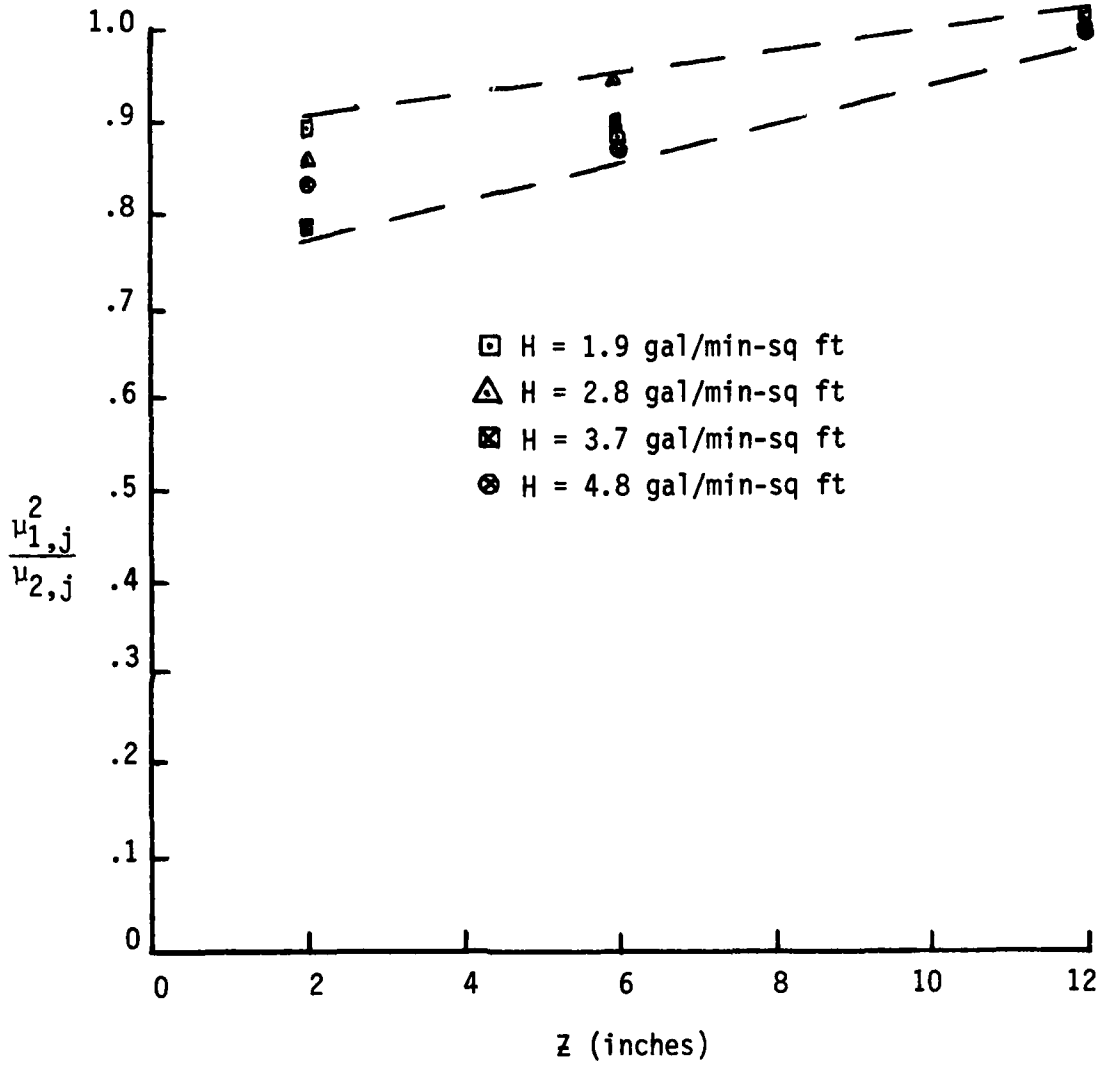

Figure 18. Effect of column length and hydraulic loading on the dimensionless ratio $\mu_{1,j}^2/\mu_{2,j}$ for binary solution of 300 ppm MIK and 300 ppm chloroform at 271.1 nm.

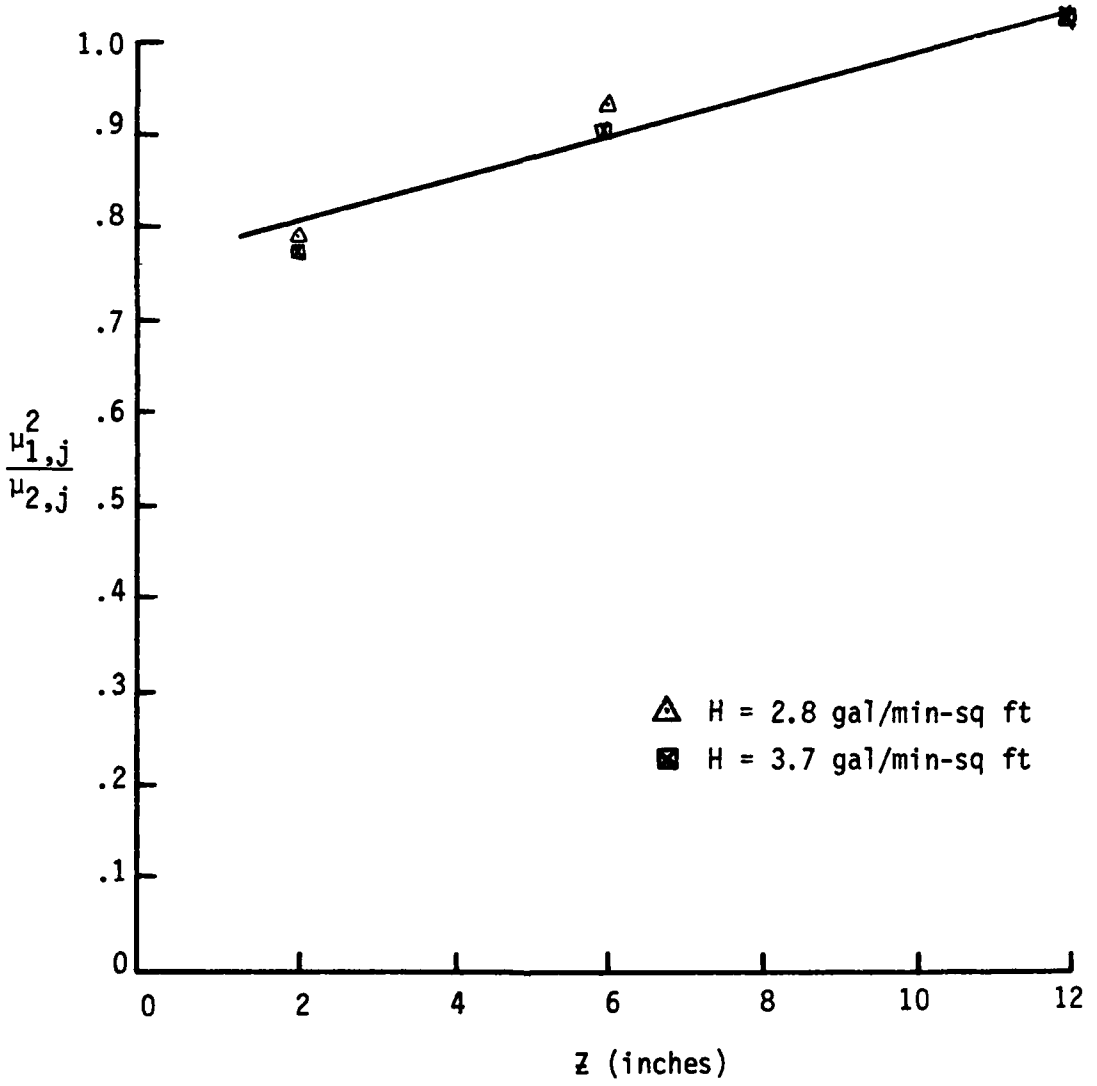

Figure 19. Effect of column length and hydraulic loading on the dimensionless ratio $\mu^2_{1,j}/\mu_{2,j}$ for 300 ppm chloroform at 211 nm.

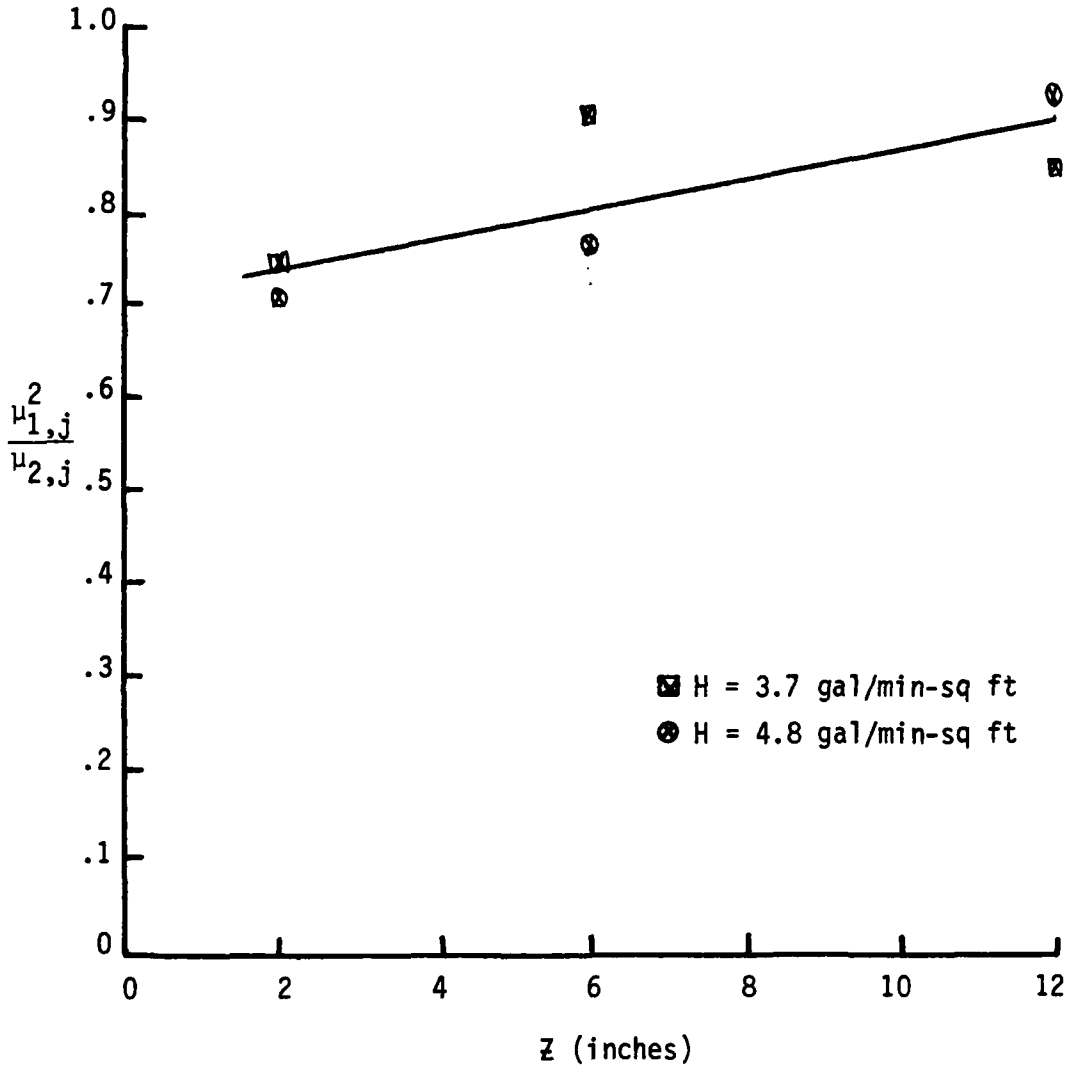

Figure 20. Effect of column length and hydraulic loading on the dimensionless ratio $\mu^2_{1,j}/\mu_{2,j}$ for binary solution of 300 ppm MIK and 300 ppm chloroform at 211 nm.

may occur faster than the mass transfer of the solute from the bulk to the surface. This would decrease the mean residence time of the system. End effects in the shorter columns caused by non-fully developed plug flow could also affect this ratio.

The results of this comparison indicate that the 2 inch column may not be the best choice for the shortest column. The scattering of the data, which occurs at the shorter column lengths, is virtually eliminated in the 12 inch columns; therefore, the 12 inch column may be a better choice for use in further research.

Equation 12 indicates not only that the ratio of the first moment squared to its correspoinding second moment should equal one but also that the ratio of the first moment squared for each column length to the second moment of the shortest column should equal the number of compartments in the system at a constant hydraulic loading. Equation 12 was applied to the data using the second moment of the 2 inch column and the first moments of 2, 6, and 12 inch columns. The results do not support this relationship, however it was found that the square root of this ratio did approximate the number of finite compartments. Table 6 compares the ratio expressed in Equation 12 to its square root for MIK. These results are consistent with the remainder of the data. Figures 21 through 24 plot the square root of this ratio as a function of column length.

To determine how well the n-FCM model would predict breakthrough curves the actual data was normalized and plotted against the dimensionless ratio $t/\bar{t}$ and compared to the calculated F(t) curve given by Equation 7 and plotted in Figure 4. Figures 25 through 28 contrast the

TABLE 6

COMPARISON OF $\frac{\mu_1^2}{\mu_2}$ AND $(\frac{\mu_1^2}{\mu_2})^{.5}$

Hydraulic Loading $\frac{\text{gal}}{\text{min-sq ft}}$	Column Length inches	$\frac{\mu_1^2}{\mu_2}$	$(\frac{\mu_1^2}{\mu_2})^{.5}$
4.8	12	0.75	0.87
	6	9.30	3.04
	2	33.89	5.82
3.7	12	0.73	0.85
	6	9.93	3.15
	2	35.65	5.97
2.8	12	0.83	0.91
	6	8.83	2.97
	2	36.51	6.04
1.9	12	0.86	0.93
	6	8.30	2.88
	2	34.70	5.89
1.0	12	0.90	0.95
	6	9.58	3.09
	2	37.29	6.11

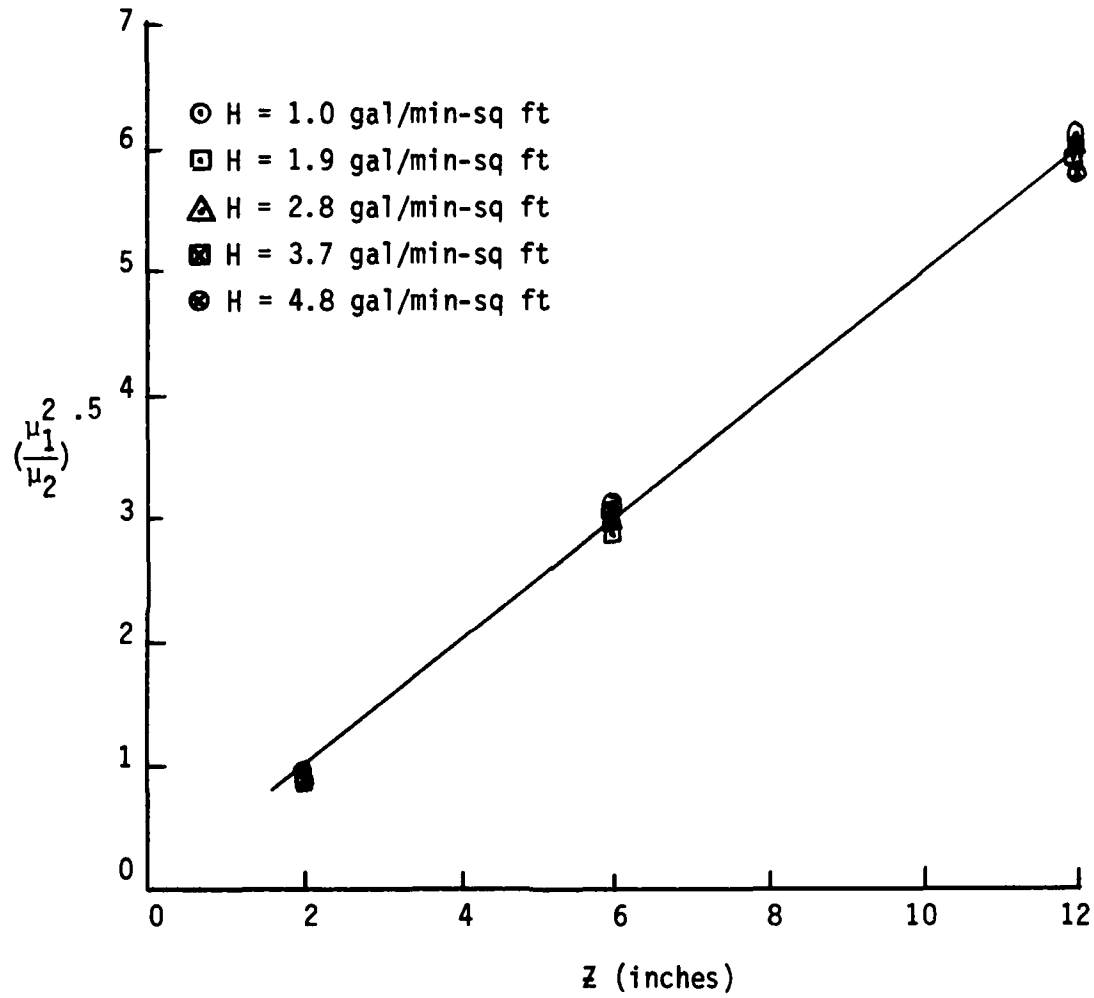

Figure 21. Effect of column length and hydraulic loading on the dimensionless ratio $(\mu_{1,j}^2/\mu_{2,2})^{.5}$ for 300 ppm MIK at 271.2 nm.

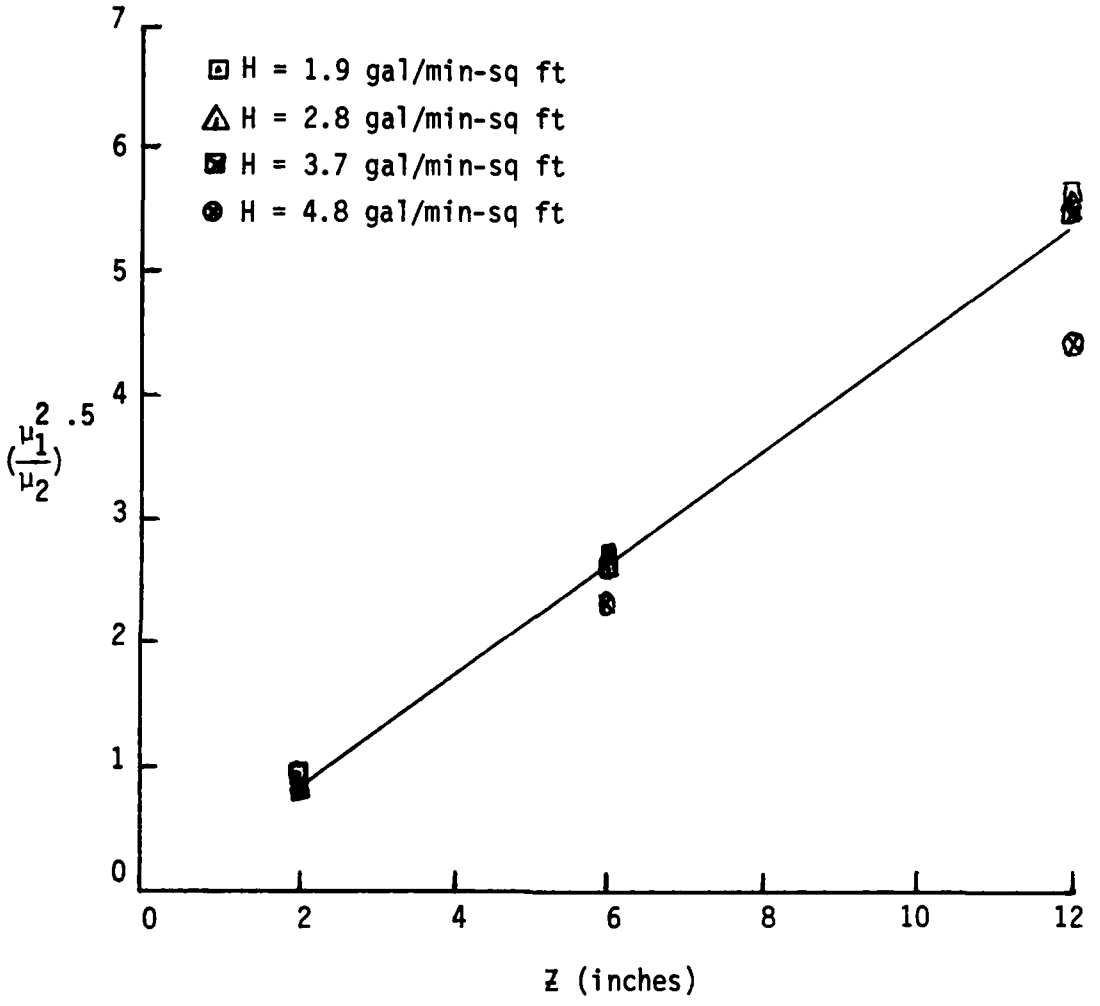

Figure 22. Effect of column length and hydraulic loading on the dimensionless ratio $(\mu^2_{1,j}/\mu_{2,2})^{.5}$ for binary solution of 300 ppm MIK and 300 ppm chloroform at 271.2 nm.

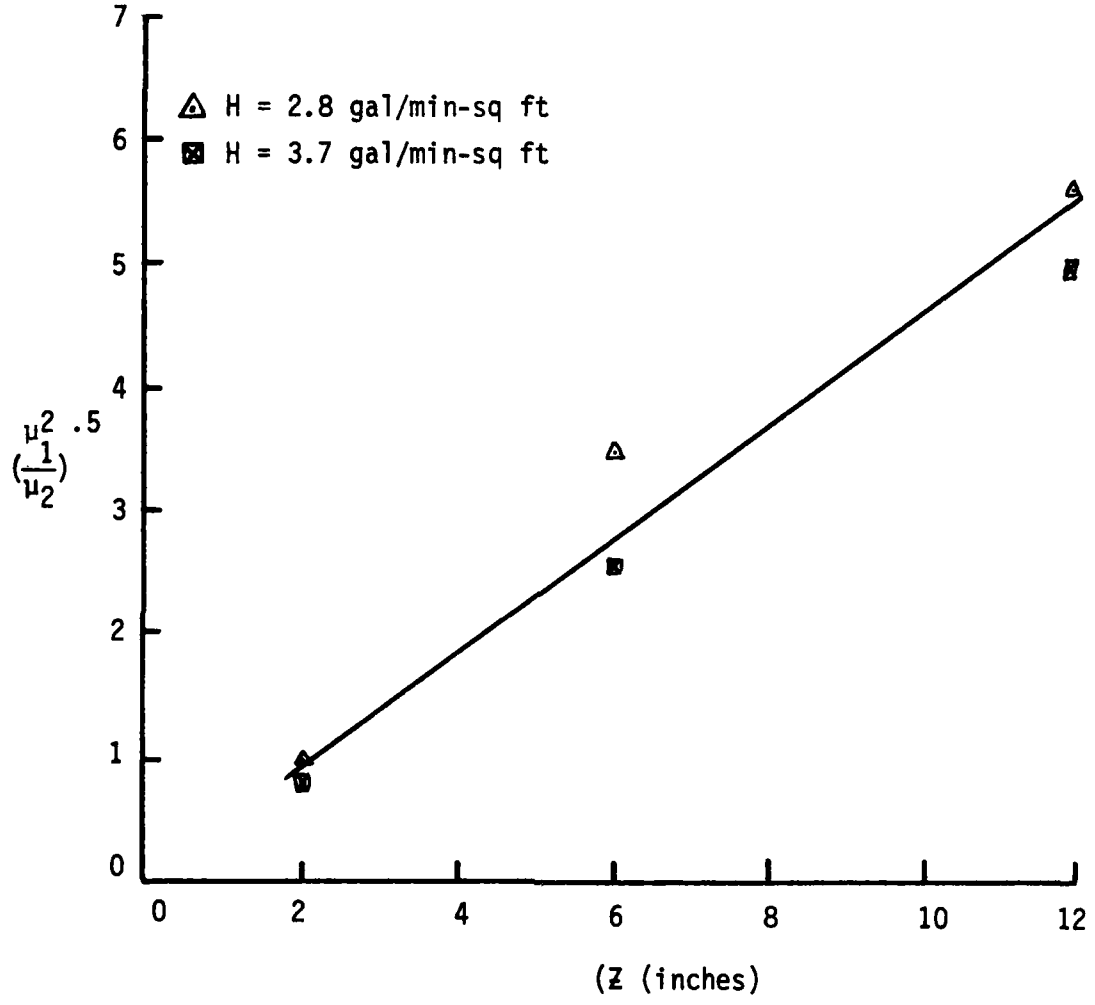

Figure 23. Effect of column length and hydraulic loading on the dimensionless ratio $(\mu_{1,j}^2/\mu_{2,2})^{.5}$ for 300 ppm chloroform at 211 nm.

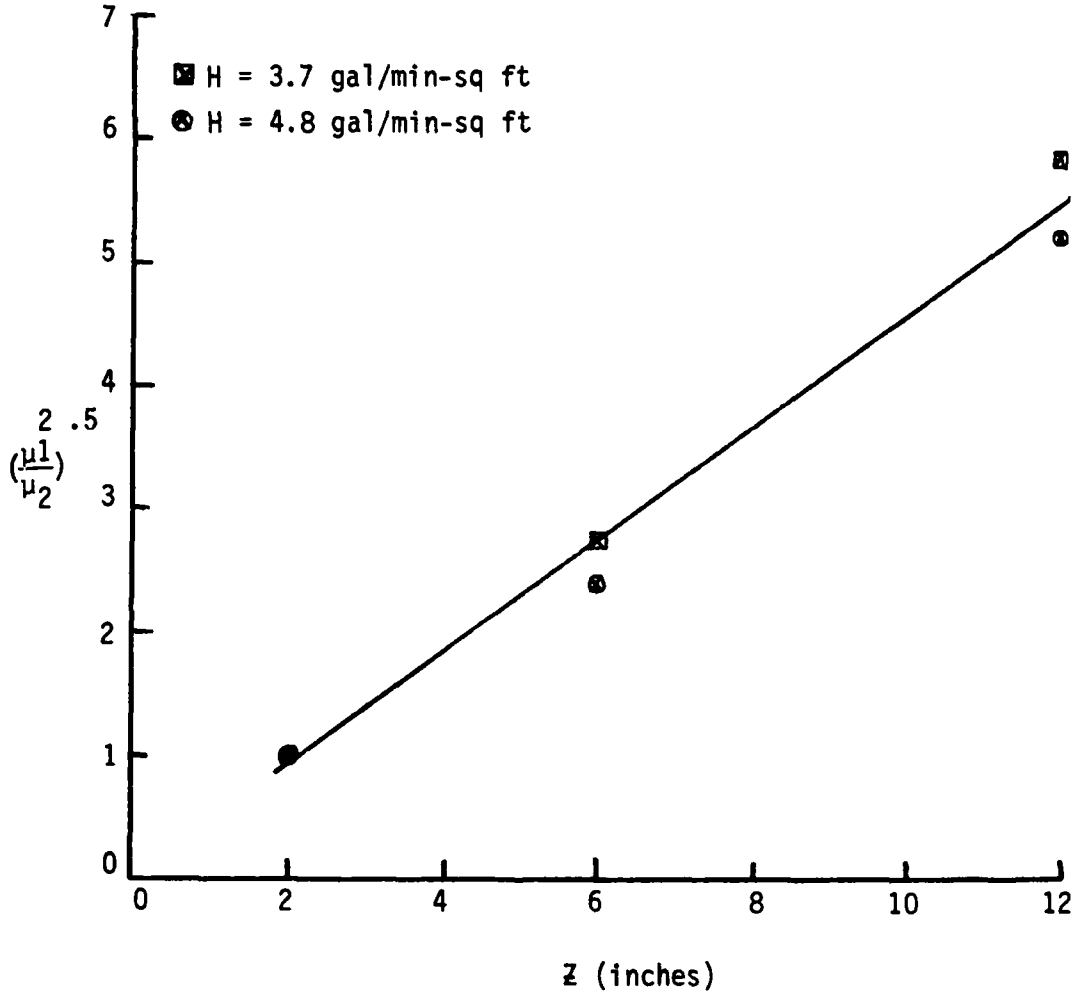

Figure 24. Effect of column length and hydraulic loading on the dimensionless ratio $(\mu^2_{1,j}/\mu_{2,2})^{.5}$ for binary solution of 300 ppm chloroform and 300 ppm MIK at 211 nm.

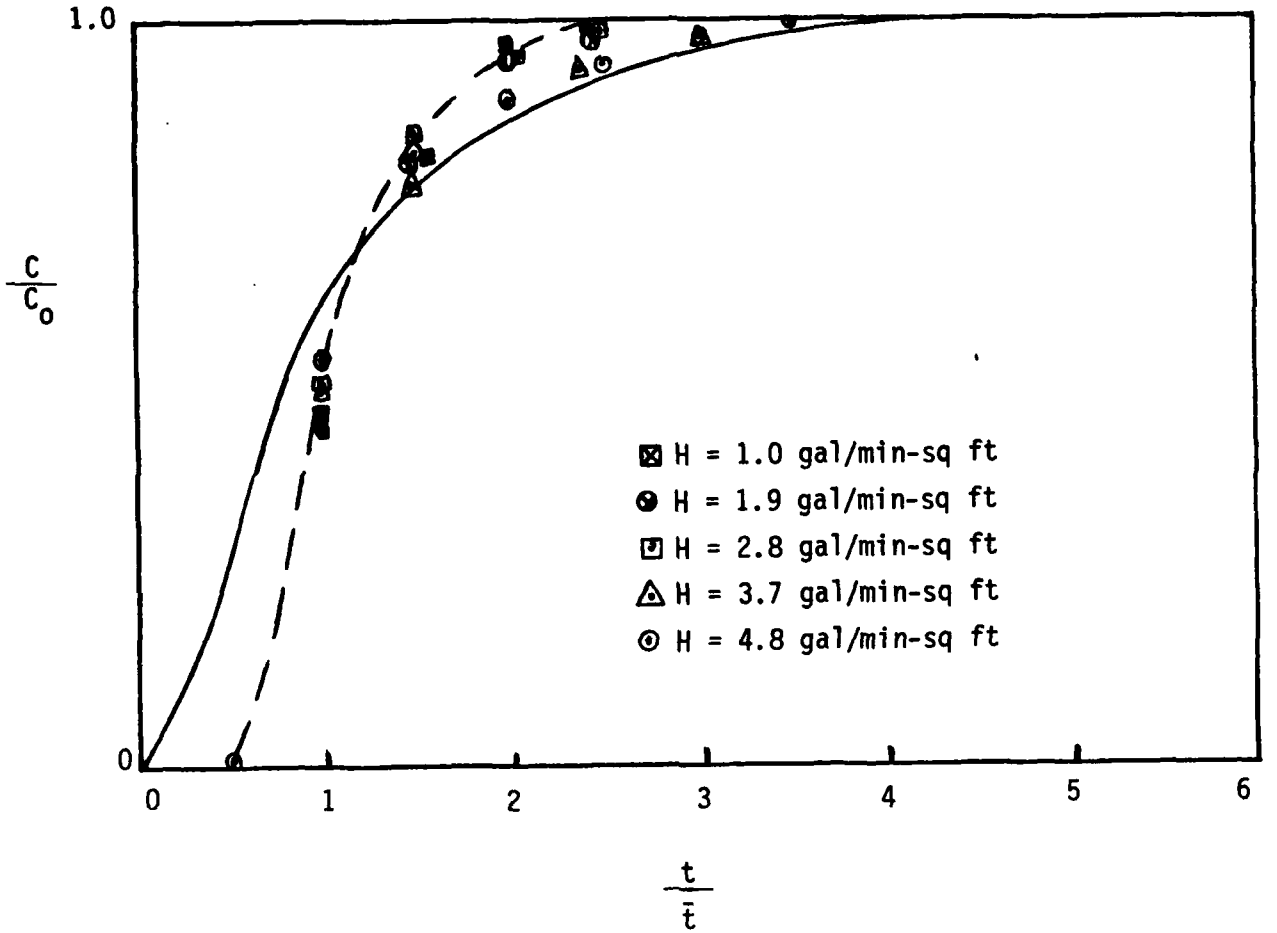

Figure 25. Breakthrough curves for 2 inch column as a function of hydraulic loading and n-FCM curve for n=1 for 300 ppm MIK at 271.2 nm.

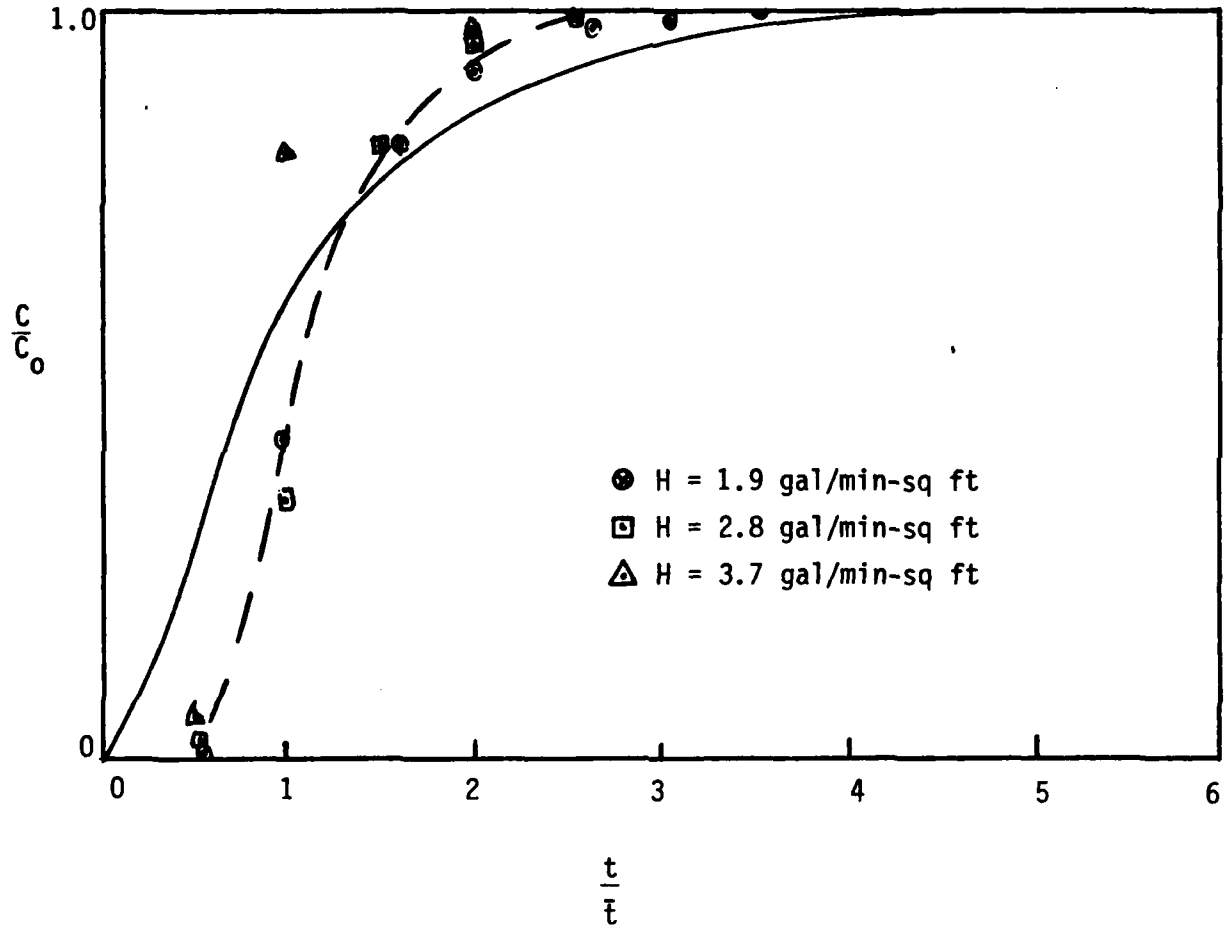

Figure 26. Breakthrough curves for 2 inch column as a function of hydraulic loading and n-FCM curve for n=1 for binary solution of 300 ppm MIK and 300 ppm chloroform at 211.2 nm.

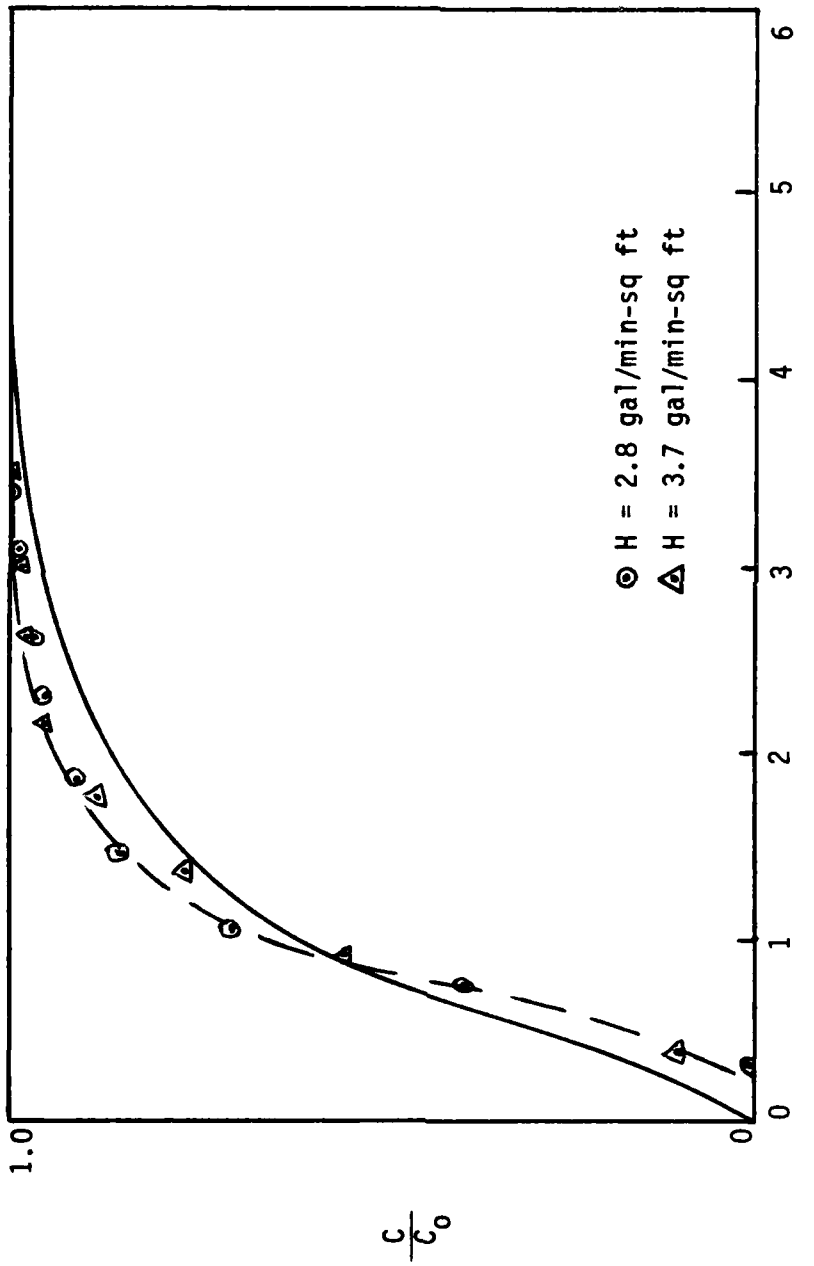

Figure 27. Breakthrough curves for a 2 inch column as a function of hydraulic loading and n-FCM curve for n=1 for 300 ppm chloroform at 211 nm.

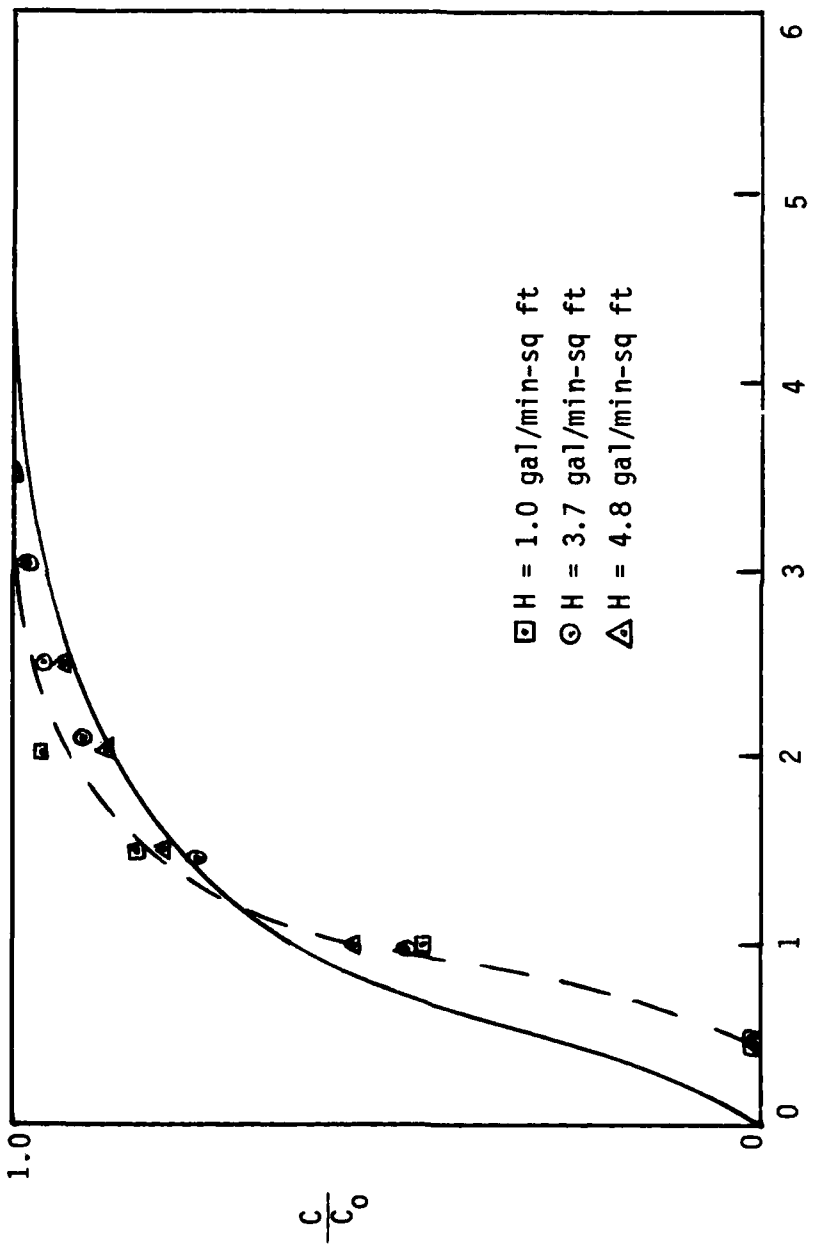

Figure 28. Breakthrough curves for 2 inch column as a function of hydraulic loading and n-FCM curve for n=1 for binary solution of 300 ppm chloroform and 300 ppm MIK at 211 nm.

actual response curve of two inch columns with a n-FCM curve where n equals one. Figures 29 through 32 do the same for six inch columns and a n-FCM curve with n equal to three. Figures 33 through 36 compare twelve inch columns and a n-FCM curve with n equal to six.

The actual data for two inch columns lags behind the calculated response curve for small values of $t/\bar{t}$ and the steeper slopes indicate that the data do not fit a F(t) curve for n equal one. This is supported by the results presented in Figures 17 through 20 where values for n calculated using Equation 12 range from 1.1 to 1.4 for 2 inch columns. The 6 inch column data also demonstrate the initial lag that may be attributed to end effects. The data appear to fit the assumed F(t) curves better than two inch column data.

For the 12 inch columns Figures 33 through 35 indicate that the actual data do not fit the assumed F(t) curve. These three sets of data fit the same order of response curve. Using Figure 4 and the general shape of the actual data points indicate a n much greater than six. On the other hand the data presented in Figure 36 fit the predicted curve well.

A possible explanation for these results is competitive adsorption. In Figures 33 and 34 MIK is the compound that is being examined. These data fit the same curve and; therefore, the effect of chloroform on MIK adsorption is negligible. In Figure 35 chloroform is the only compound present and its response curve is congruent with those in Figures 33 and 34. In Figure 36 the chloroform concentration is being monitored in the presence of MIK. These data fit the assumed response curve. This result indicates that adsorption of the chloroform is

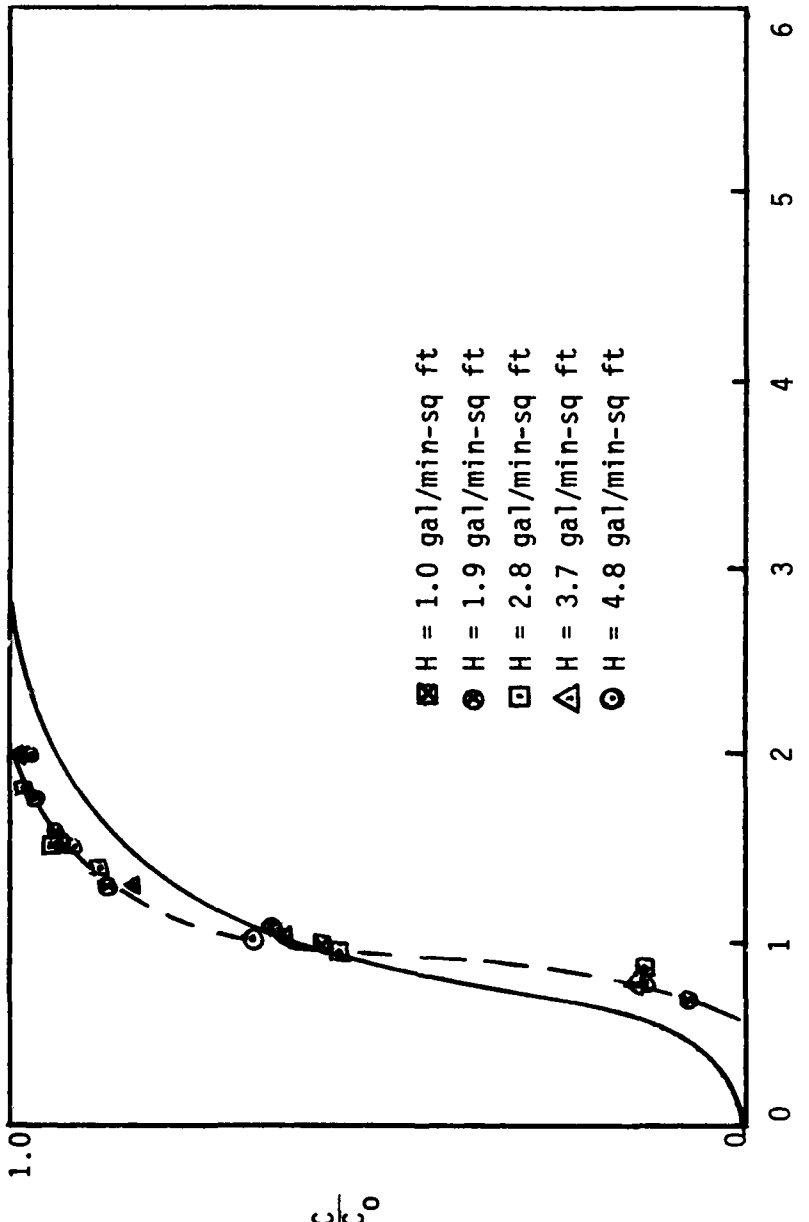

Figure 29. Breakthrough curves for 6 inch column as a function of hydraulic loading and n-FCM curve for n=3 for 300 ppm MIK at 271.2 nm.

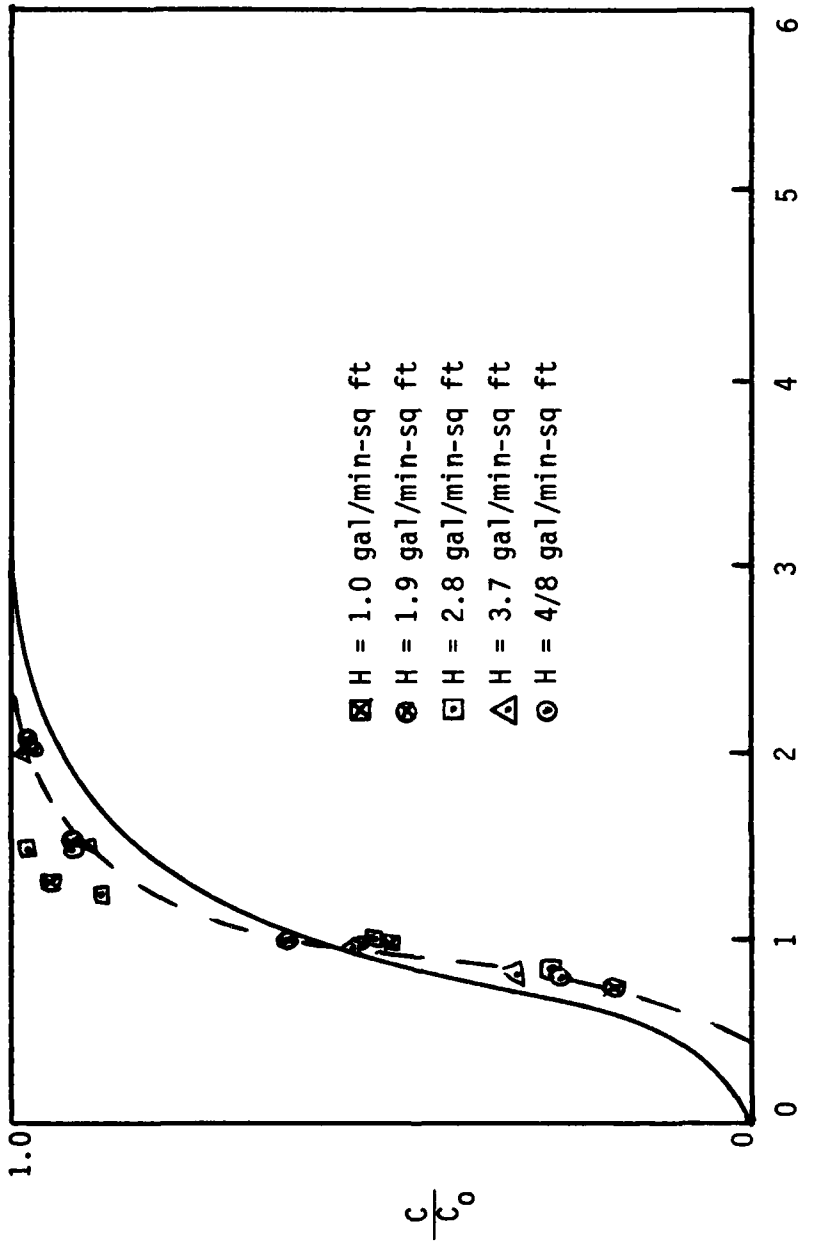

Figure 30. Breakthrough curves for 6 inch column as a function of hydraulic loading and n-FCM curve for n=3 for binary solution of 300 ppm chloroform and 300 ppm MIK at 271.2 mm.

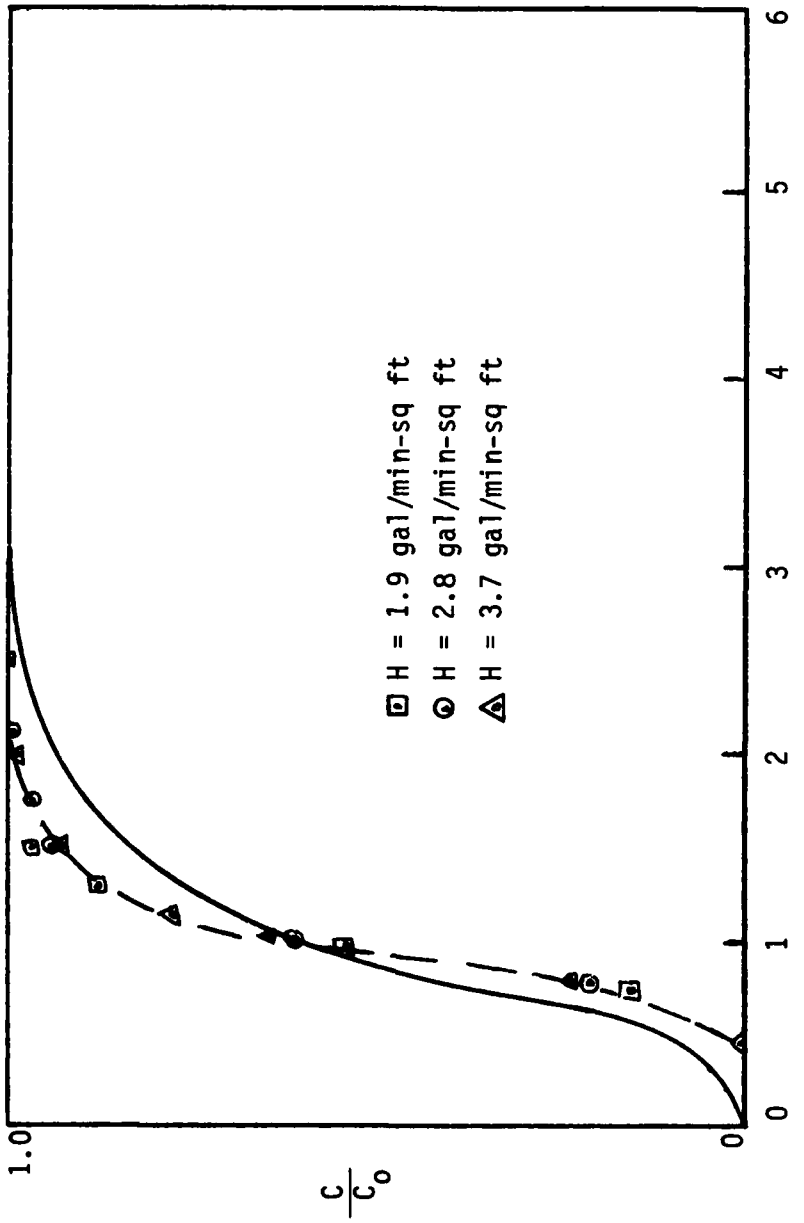

Figure 31. Breakthrough curves for 6 inch column as a function of hydraulic loading and n-FCM curve for n=3 for 300 ppm chloroform at 211 nm.

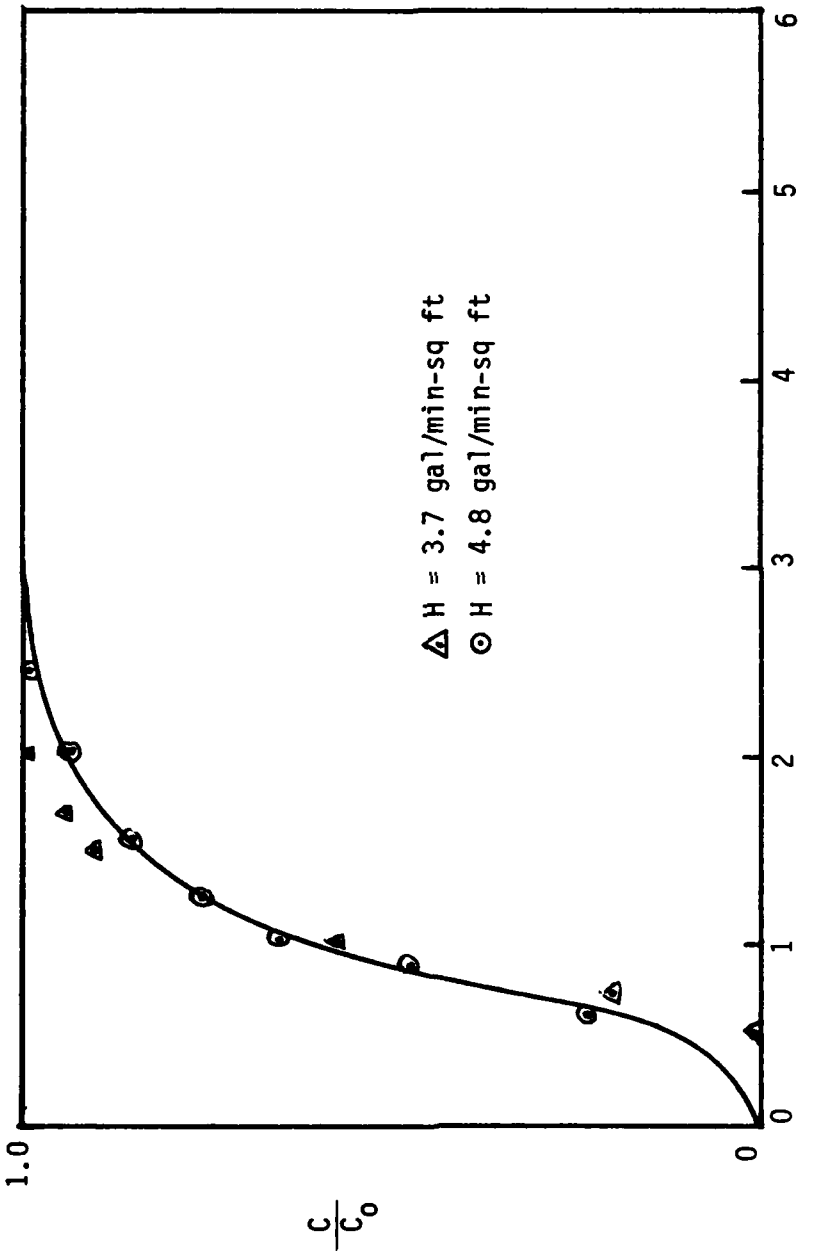

Figure 32. Breakthrough curves for 6 inch column as a function of hydraulic loading and n-FCM curve for n=3 for binary solution of 300 ppm chloroform and 300 ppm MIK at 211 nm.

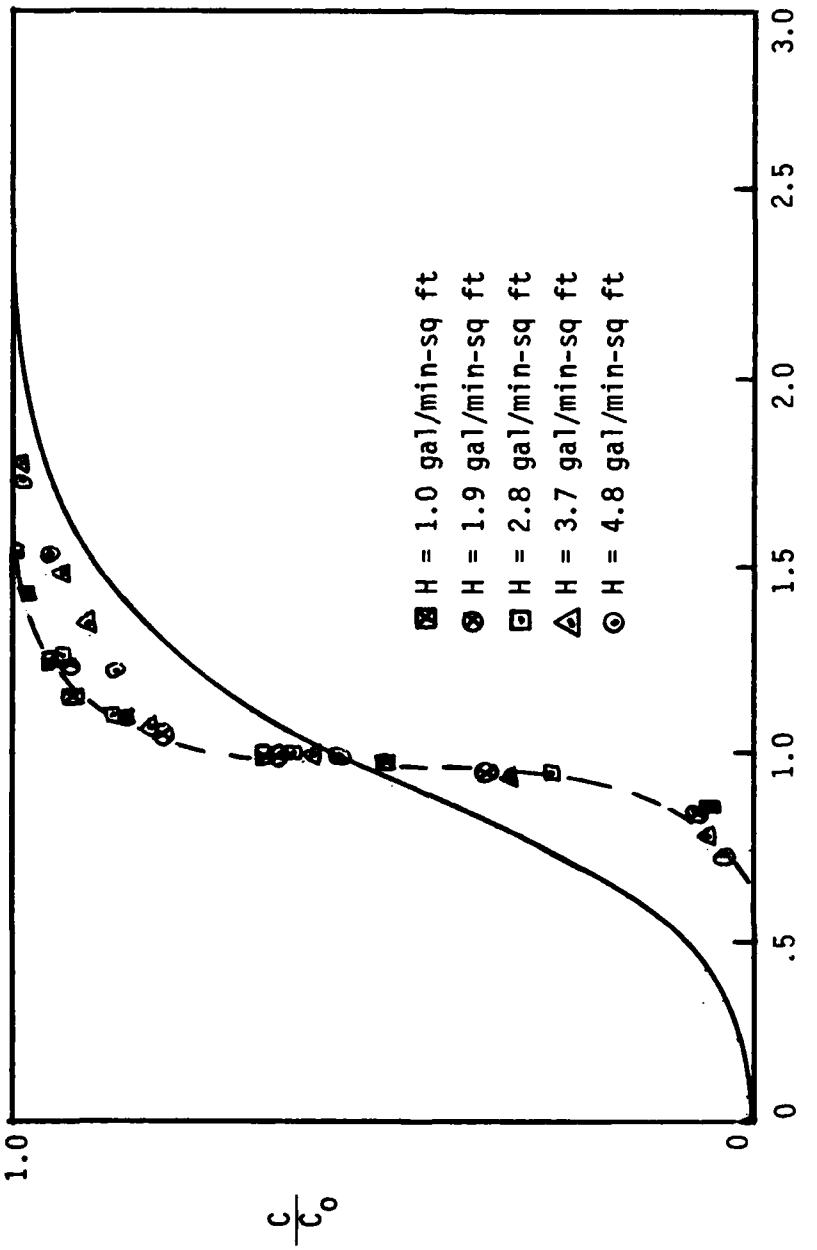

Figure 33. Breakthrough curves for 12 inch column as a function of hydraulic loading and n-FCM curve for n=6 for 300 ppm MIK at 271.2 nm.

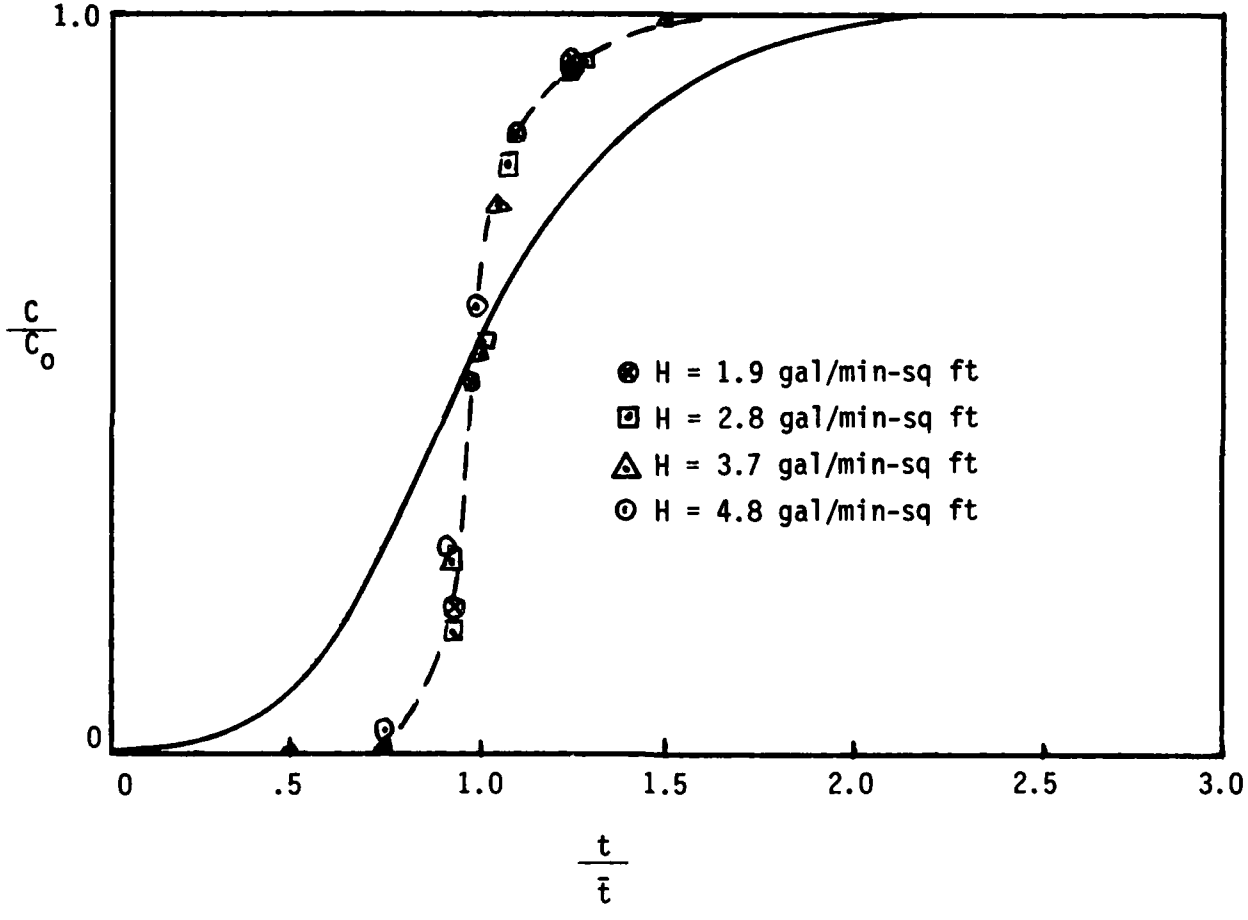

Figure 34. Breakthrough curves for 12 inch column as a function of hydraulic loading and n-FCM curve for n=6 for binary solution of 300 ppm MIK and 300 ppm chloroform at 271.2 nm.

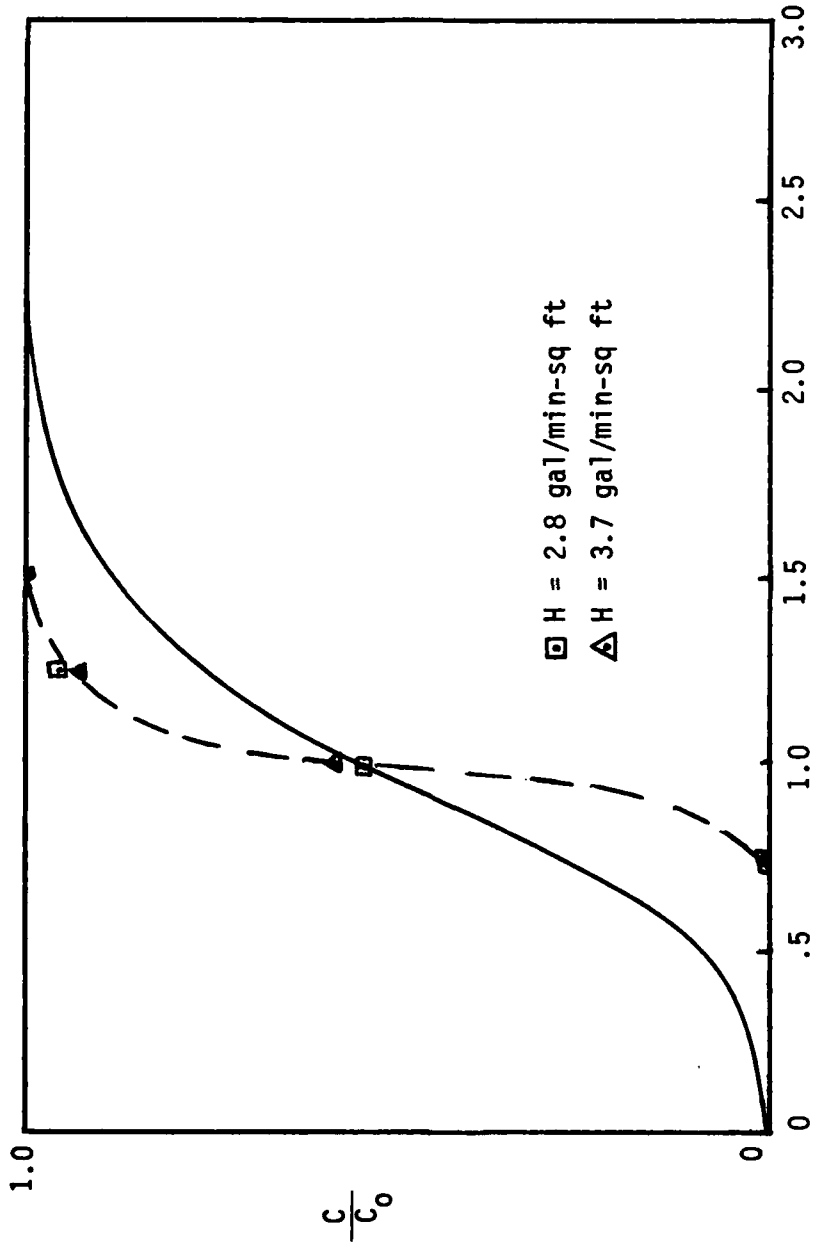

Figure 35. Breakthrough curves for 12 inch column as a function of hydraulic loading and n-FCM curve for n=6 for 300 ppm chloroform at 211 nm.

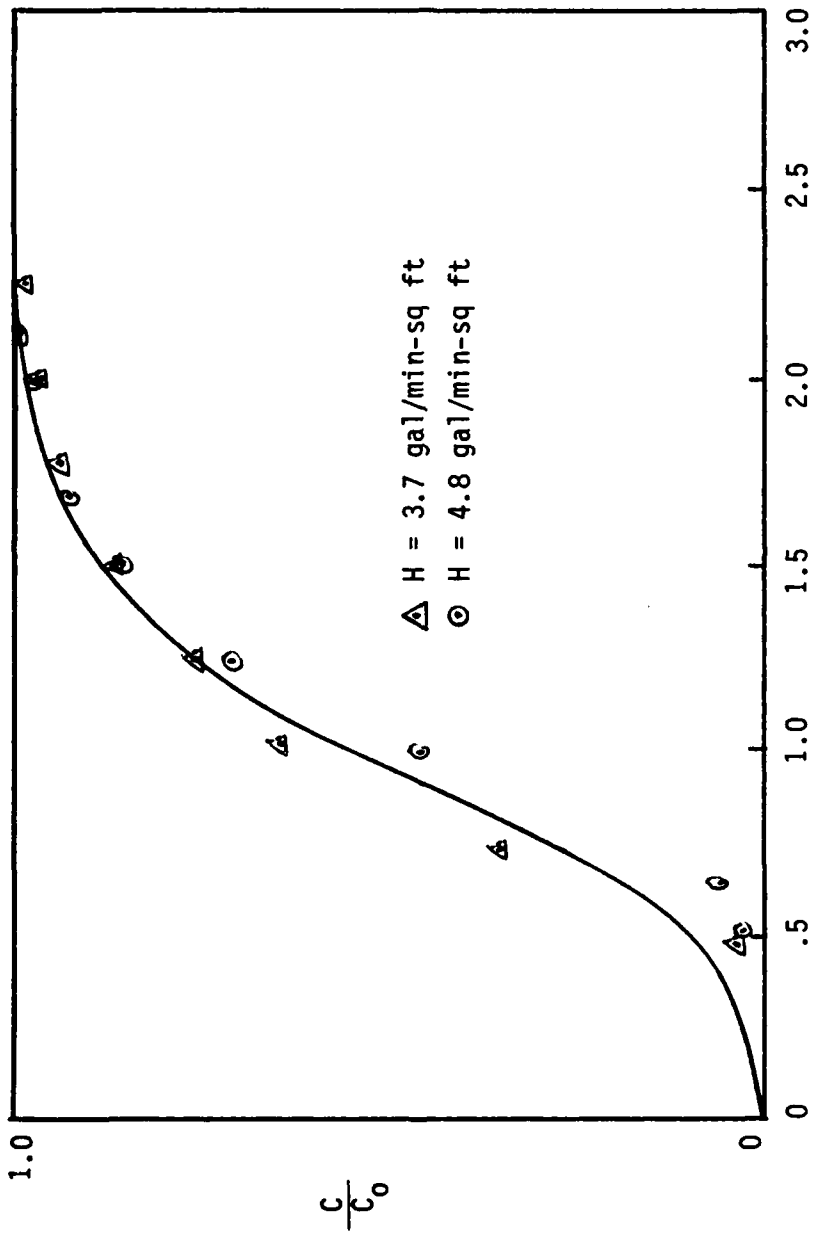

Figure 36. Breakthrough curve for 12 inch column as a function of hydraulic loading and n-FCM curve for n=6 for binary solution of 300 ppm chloroform and 300 ppm MIK at 211 nm.

hindered by the presence of MIK and the response curve is for a system with fewer finite compartments.

Figure 37 and Table 7 illustrate the relationship between column diameter and the first moment. The column diameter does not appear to influence the first moment. The first moment is essentially constant for each series of runs conducted at a fixed hydraulic loading and varied column diameter.

Figure 38 represents the dimensionless ratio of the first moment squared to the second moment for six inch columns. The data are plotted versus hydraulic loading. The results indicate that the column diameter has little effect on this ratio and that increased hydraulic loads cause a decrease in this ratio. This observation supports the earlier contention that as the physical transport is increased adsorption is decreased.

TABLE 7

COMPARISON OF TUBE DIAMETER TO PARTICLE DIAMETER
FOR MIK IN 6 INCH COLUMNS AT VARIOUS FLOW RATES

Hydraulic Loading gal/min-sq ft	Tube Diameter inches	First Moment min	Diameter Ratios
4.8	.25	16.1	15.0:1
	.375	15.4	25.4:1
3.7	.25	20.6	15.0:1
	.375	20.3	25.4:1
	.50	20.6	35.8:1
2.8	.25	27.9	15.0:1
	.375	25.1	25.4:1
	.50	27.6	35.8:1
1.9	.25	38.0	15.0:1
	.375	41.1	25.4:1
	.50	42.9	35.8:1
1.0	.25	75.7	15.0:1
	.375	75.0	25.4:1
	.50	74.2	35.8:1

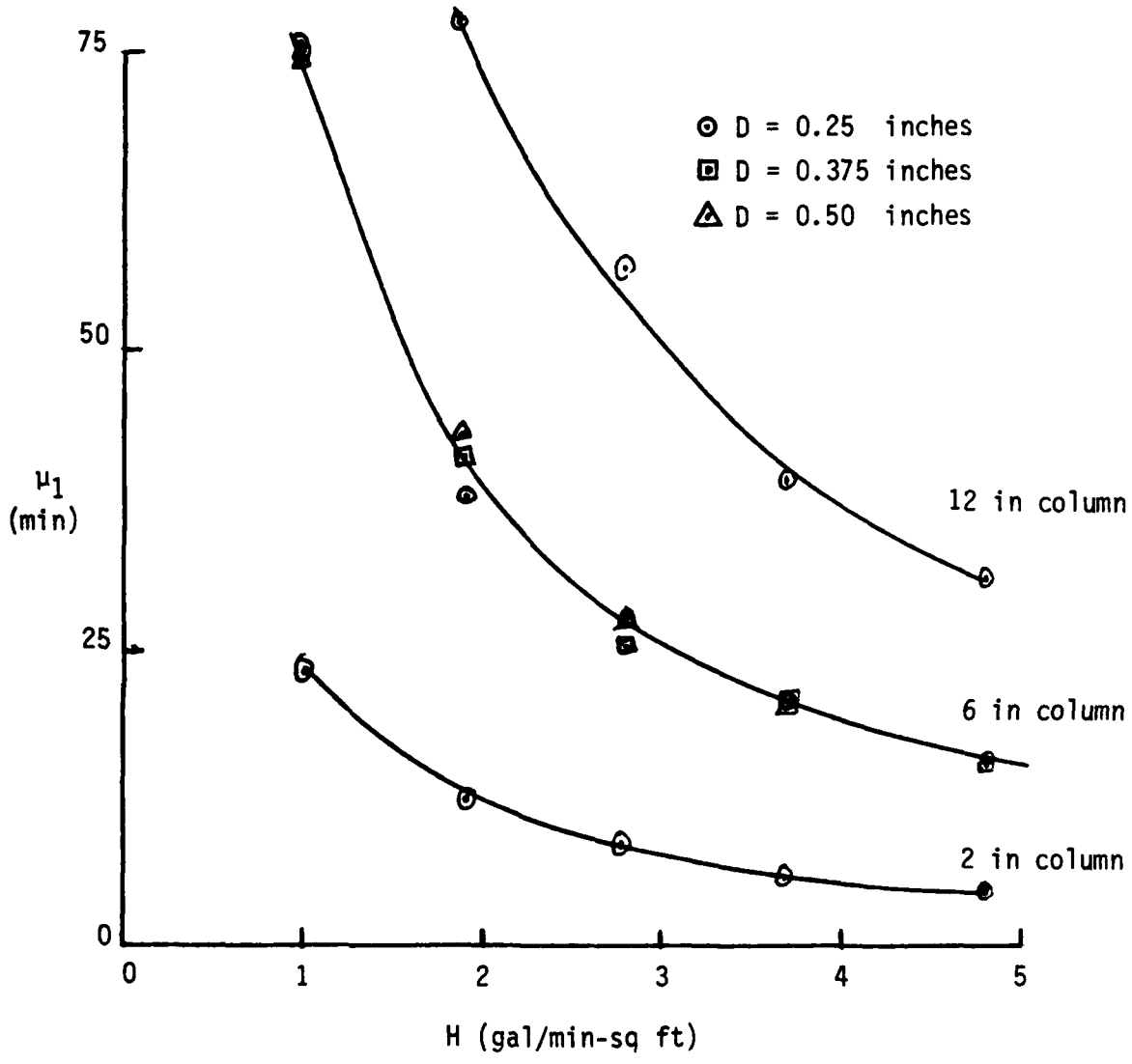

Figure 37. Effect of column diameter and hydraulic loading on first moment of 300 ppm MIK at 271.2 nm.

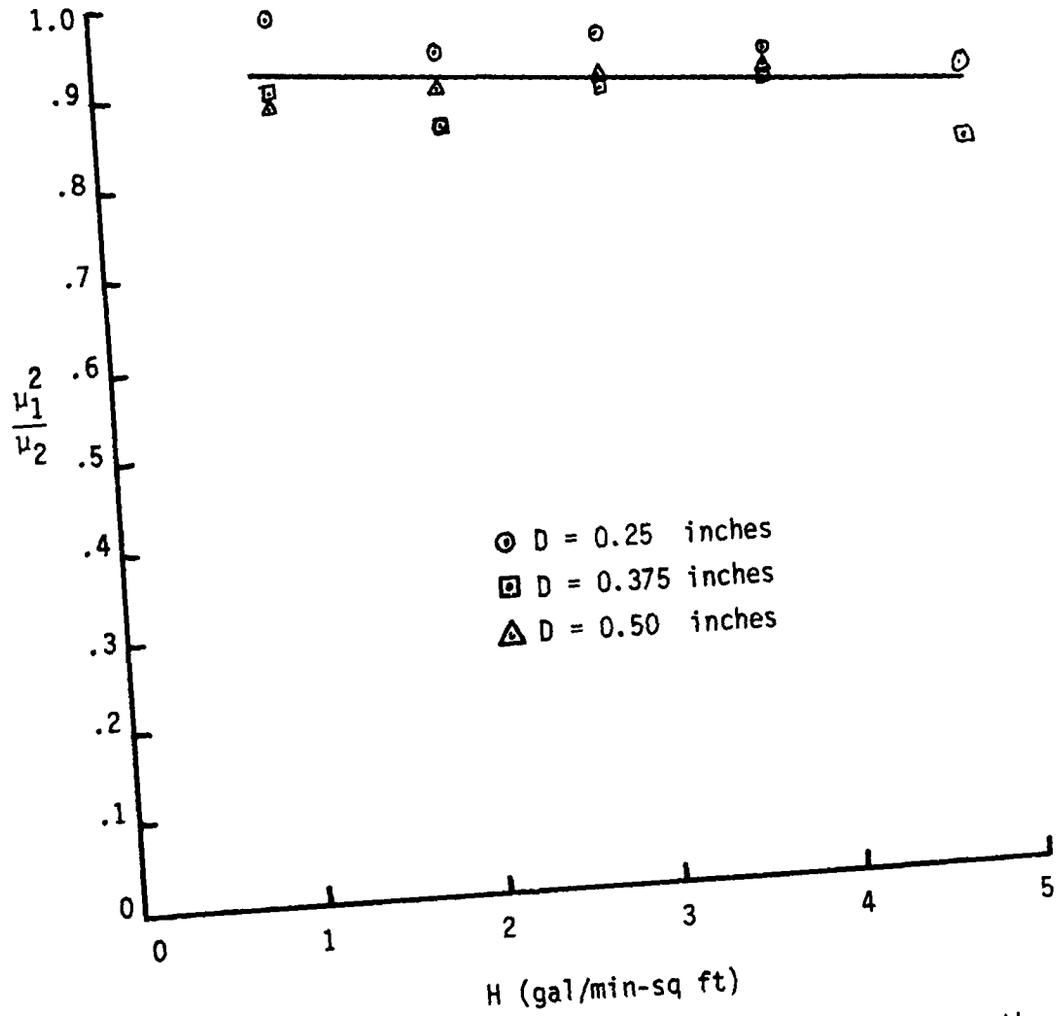

Figure 38. Effect of column diameter and hydraulic loading on the dimensionless ratio μ_1^2/μ_2 for 300 ppm MIK at 271.2 nm.

CHAPTER VI

CONCLUSION AND RECOMMENDATION

The results obtained during this research indicate that:

1. The experimental data do not fully support the use of the n-FCM model with either single or binary solute solutions.
2. The method of moments provides a means of calculating the mean residence time and variance from an actual response curve.
3. Column diameter, over the limited range studied, when related to a fixed particle diameter does not influence the adsorption process.
4. The presence of MIK interferes with the adsorption of chloroform from binary solution.

It is recommended that additional research in the following areas be conducted:

1. Further data should be taken for binary systems.
2. Data taken on experimental setups similar to the one used in this research should be done at a single UV wavelength rather than at two. The binary should be treated as a pseudo single solute system. In an actual design process this may prove to work better than trying to treat the solutes separately.

3. Further studies concerning the ratio of column to particle diameter should be conducted to include using larger column diameters, different lengths, and varied particle diameters with a fixed column diameter.

AD-A141 483 APPLICATION OF THE FINITE COMPARTMENT MODEL OF CARBON ADSORPTION TO BINARY SYSTEMS(U) ARMY MILITARY PERSONNEL CENTER ALEXANDRIA VA T R NOREEN MAY 84 2/2

UNCLASSIFIED F/G 7/4 NL

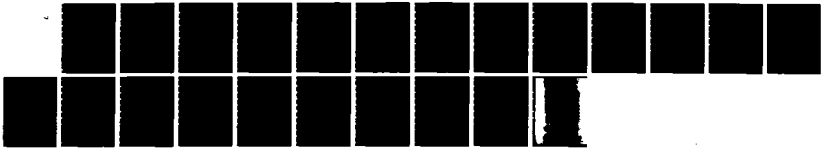

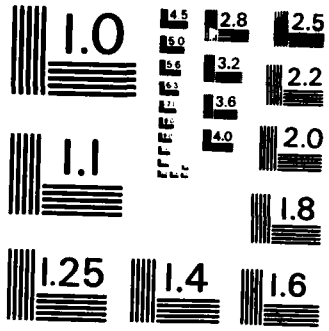

APPENDIX A

EQUILIBRIUM ISOTHERM CALCULATIONS

APPENDIX A

EQUILIBRIUM ISOTHERM CALCULATIONS

Table 8 displays the liquid concentrations, in ppm by volume, of MIK used in isotherm shaker bath studies.

TABLE 8

LIQUID CONCENTRATIONS

Flask Number	Initial Concentration (ppm)	Equilibrium Concentration (ppm)	Volume of Liquid (cm)
1	100	18	200
2	200	53	200
3	300	123	200

Equilibrium solid concentration (gram MIK/gram carbon), is the ratio of the change in liquid concentration to the amount of carbon present in each flask, 2 grams.

Example:

For flask # 1

$$Q_e = \frac{(\text{grams MIK})_{\text{initial}} - (\text{grams MIK})_{\text{final}}}{\text{grams of carbon}}$$

$$Q_e = \frac{(.1592 - .0286)gm}{2\ gm} = .0652\ gm/gm$$

Table 9 shows the equilibrium solid concentration in each flask.

TABLE 9

EQUILIBRIUM SOLID CONCENTRATION

Flask Number	Carbon (grams)	Equilibrium Solid Concentration (gm/gm)
1	2	0.0652
2	2	0.1167
3	2	0.1397

This data is fit to the Freundlich isotherm in Figure 39. A straight line connects these data by method of least squares. Values of the Freundlich constants are K = 0.00246 and n = 0.7153. Figures 40 and 41 display the Freundlich plots for chloroform and the binary mixture.

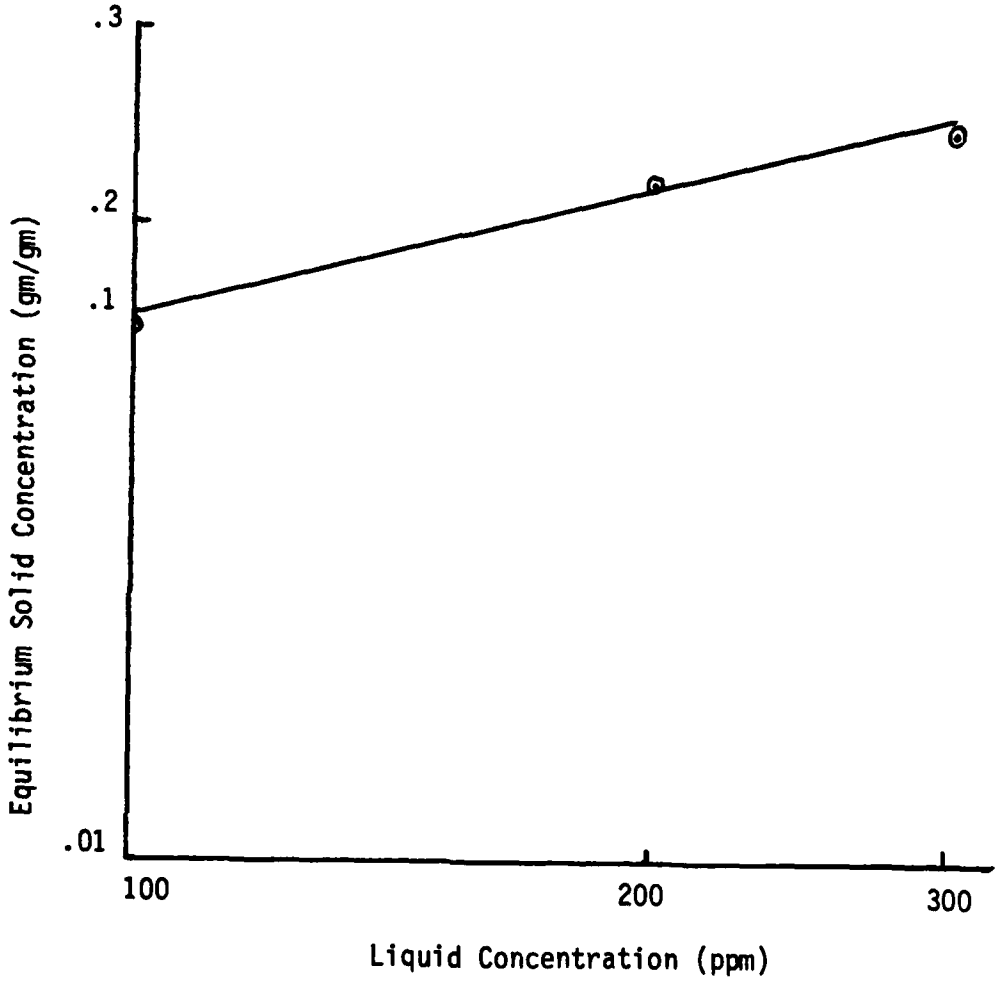

Figure 39. Freundlich isotherm for MIK solutions.

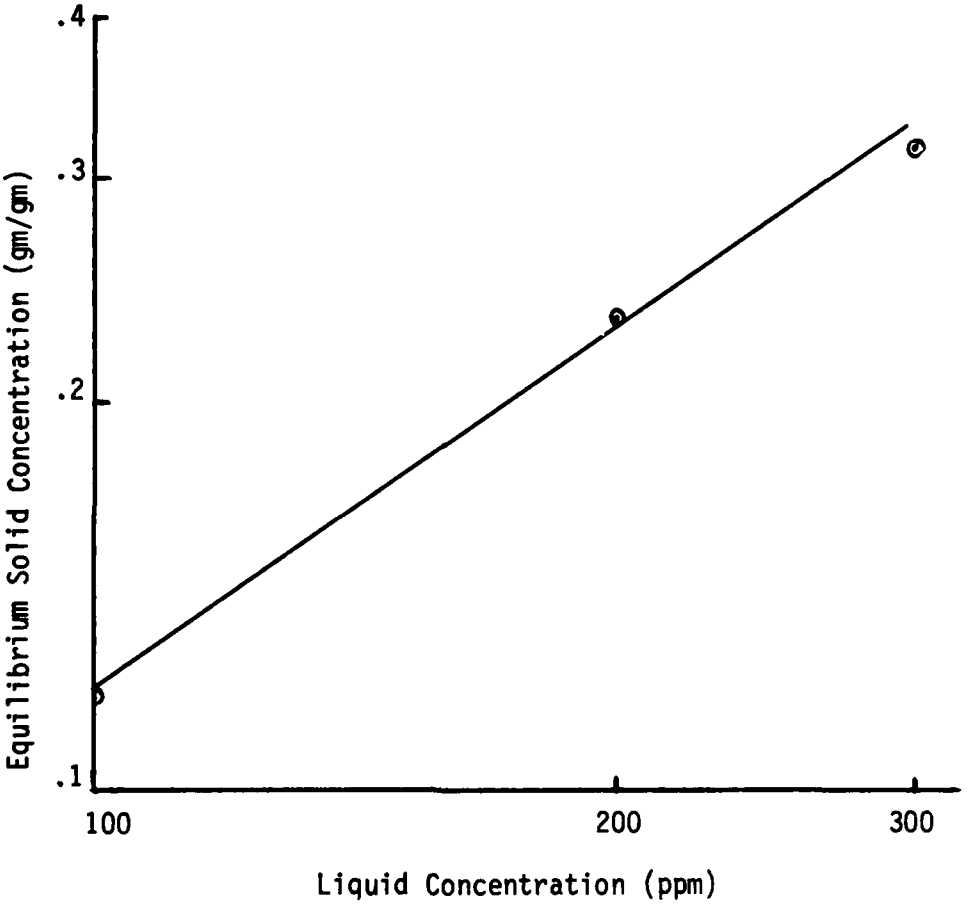

Figure 40. Freundlich isotherm for chloroform solutions.

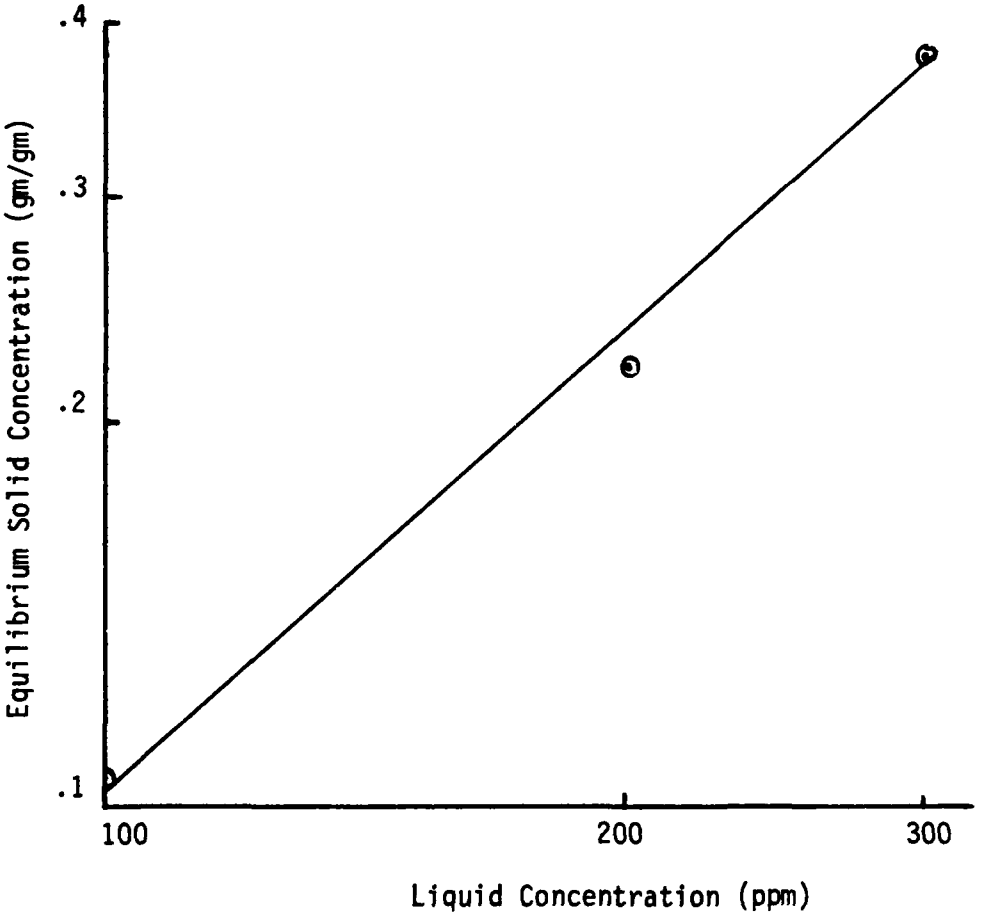

Figure 41. Freundlich isotherm for binary solution of chloroform and MIK.

APPENDIX B

CALCULATION OF MOMENTS

APPENDIX B

CALCULATION OF MOMENTS

Equations 9 through 11 in Chapter III can be readily integrated in the following expressions:

$$\mu_i = [(1 - \frac{C_i}{C_o}) \Delta t] \quad (16)$$

$$\mu_2 = [(1 - \frac{C_i}{C_o}) t_i \Delta t] \quad (17)$$

$$\mu_3 = [(1 - \frac{C_i}{C_o}) t_i^2 \Delta t] \quad (18)$$

where:

t_i = time, min.

$1 - \frac{C_i}{C_o}$ = normalized concentration.

Δt = selected time interval for integration, min.

Response curves are evaluated and the concentration versus time data is tabulated. These data are read into a file from which the computer will calculate the moments. The results of these calculations are found in Tables 10 through 15 in this appendix. The computer program is listed in Appendix C.

TABLE 10

MOMENTS FOR 300 PPM MIK AT 271.2 NM

Hydraulic Loading gal/min-Sq ft	Z inches	μ_1 min	μ_2 min	μ_3 min
4.8	12	30.66	985.74	33480.6
	6	16.06	292.24	6164.9
	2	4.57	27.74	220.0
3.7	12	39.05	1585.96	67262.1
	6	20.61	465.31	11654.0
	2	5.59	42.77	433.3
2.8	12	56.66	3281.87	195067.6
	6	27.87	827.93	26491.2
	2	8.55	87.94	1084.9
1.9	12	77.72	6175.73	503987.0
	6	38.02	1551.85	68816.0
	2	12.24	174.05	2891.5
1.0	12	149.24	22565.16	3466338.0
	6	75.66	5837.65	460072.5
	2	23.22	597.29	17216.6

TABLE 11

MOMENTS FOR BINARY SOLUTION OF 300 PPM MIK AND 300 PPM CHLOROFORM AT 271.2 NM

Hydraulic Loading gal/min-sq ft	Z inches	μ_1 min	μ_{2_2} min^2	μ_{3_3} min^3
4.8	12	23.69	575.23	14360.0
	6	12.56	182.65	3065.2
	2	4.91	29.01	208.6
3.7	12	31.79	1029.79	34046.8
	6	15.32	263.74	5099.5
	2	5.07	32.98	280.6
2.8	12	45.02	2059.93	95913.9
	6	21.32	476.44	11164.7
	2	7.41	64.05	642.4
1.9	12	64.05	4159.49	274365.7
	6	29.75	1009.66	40515.4
	2	10.61	125.65	1675.9
1.0	12	61.81	3904.61	252409.5
	6	61.15	3812.4	24535.10
	2	6.61	46.96	360.42

TABLE 12

MOMENTS FOR 300 PPM CHLOROFORM AT 211 NM

Hydraulic Loading gal/min-sq ft	Z inches	μ_1 min	μ_2 min^2	μ_3 min^3
4.8	6	30.48	1104.48	47660
3.7	12	78.36	6282.72	517519
	6	40.12	1781.14	88712
	2	13.68	242.64	5735
2.8	12	102.18	10604.16	1119510
	6	63.01	4271.44	311150
	2	16.14	331.21	8929
1.9	6	84.47	7446.96	685395
1.0	6	146.41	21870.0	3351577

TABLE 13

MOMENTS FOR BINARY SOLUTION OF 300 PPM MIK AND 300 PPM CHLOROFORM AT 211 NM

Hydraulic Loading gal/min-sq ft	Z inches	μ_1 min	μ_2 min^2	μ_3 min^3
4.8	12	41.28	1848.85	89274.5
	6	18.98	474.12	14715.3
	2	6.71	63.62	785.3
3.7	12	63.62	4831.21	434308.0
	6	29.95	995.54	36549.0
	2	9.37	118.27	1925.0
2.8	6	31.46	1230.34	57695.0
1.0	6	107.18	11991.24	1401464.0
	2	29.75	1007.78	38409.0

TABLE 14

MOMENTS FOR 300 PPM MIK IN 3/8 x 6 IN
COLUMN AT 271.2 NM

Hydraulic Loading gal/min-sq ft	μ_1 min	μ_2 min^2	μ_3 min^3
4.8	15.37	294.06	6876.0
3.7	20.26	463.84	12128.0
2.8	25.09	710.63	22970.0
1.9	41.11	1982.68	112797.0
1.0	75.02	6234.34	585453.0

TABLE 15

MOMENTS FOR 300 PPM MIK IN 1/2 x 6 IN COLUMN AT 271.2 NM

Hydraulic Loading gal/min-sq ft	μ_1 min	μ_2 min^2	μ_3 min^3
3.7	20.57	471.34	12101.0
2.8	27.64	857.66	30067.0
1.9	42.93	2058.53	112371.0
1.0	74.19	6231.24	605097.0

APPENDIX C

SAMPLE COMPUTER PROGRAM

APPENDIX C

SAMPLE COMPUTER PROGRAM

The following program is written in BASIC for the Commodore 64 microcomputer. The program uses the trapezpoid rule to numerically integrate Equations 16 through 18.

```
10 DIM Y(75),T(75),X(76)
20 REM THIS PROGRAM CALCULATES THE FIRST, SECOND AND THIRD MOMENTS
30 REM ENTER THE WIDTH, TIME INTERVAL, AND THE NUMBER OF DATA POINTS
50 INPUT"ENTER H";H
70 GOSUB660  :REM DATA ENTRY
80 GOSUB840  :REM DATA CALCULATION
90 GOSUB290  :REM DATA CORRECTION
100  GOSUB290  :REM CALCULATION OF FIRST MOMENT
110  GOSUB390  :REM CALCULATION OF SECOND MOMENT
120  GOSUB480  :REM CALCULATION OF THIRD MOMENT
130  GOSUB570  :REM PRINT HARD COPY DATA
140 INPUT"ENTER Y TO CONTINUE";C$
150 IF C$="N" THEN 640
160 GOTO40
250 FOR I=1 TO N
260 T(I)=H*(I-1)
270 NEXT I
280 RETURN
290 OPEN 2,4:CMD2
300 PRINT"RUN NUMBER:";U$:PRINT
310 U1=0
320 FOR I=2 TO N-1
330 U1=U1+Y(I)
340 NEXT I
350 U1=H*(U1+.5*(Y(1)+Y(N)))
360 PRINT"U1=";U1
370 PRINT#2," ":CLOSE2
380 RETURN
390 OPEN2,4:CMD2
400 U2=0
410 FOR I=2 TO N-1
420 U2=U2+T(I)*Y(I)
430 NEXT I
440 U2=2*H*(U2+.5*(Y(1)*T(1)+Y(N)*T(N)))
450 PRINT "U2=";U2
460 PRINT#2," ":CLOSE2
470 RETURN
480 OPEN2,4:CMD2
490 U3=0
500 FOR I=1 TO N-1
510 U3=U3+Y(I)*T(I)^2
520 NEXT I
530 530 U3=3*H*(U3+.5*(Y(1)*T(1)^2+Y(N)*T(N)^2))
540 PRINT"U3=";U3
550 PRINT#2," ":CLOSE2
560 RETURN
570 PRINT
580 OPEN2,4:CMD2
590 FOR I=1 TO N
```

```
600 PRINT "Y(";I;")=";Y(I);"T=";T(I)
610 NEXT I
620 PRINT#2,"":CLOSE2
630 RETURN
640 PRINT"END"
650 END
660 REM INPUT DATA
670 INPUT"NUMBER OF DATA PAIRS";N
680 PRINT"IS DATA TO BE READ FROM A FILE (Y OR N)?"
690 INPUT V$
700 IF V$<>"Y" THEN790
710 INPUT"FILE NAME";U$
720 OPEN15,8,15
730 OPEN5,8,5,"@0:"+U$+",S,R"
740 FOR I=1 TO N
750 INPUT#5,Y(I)
760 NEXT I
770 CLOSE5:CLOSE15
780 GOTO830
790 FOR I=1 TO N
800 PRINT I;
810 INPUT"DATA Y";Y(I)
820 NEXT I
830 RETURN
840 PRINT" #";TAB(t);"T VALUE";TAB(15);"Y VALUE"
850 FOR I=1 TO N
860 PRINT I;TAB(5);T(I);TAB(15);Y(I)
870 NEXT I
880 INPUT"ARE ALL DATAOK? Y OR N";A$
890 PRINT:PRINT
900 IF A$="Y" THEN960
910 T=0
920 INPUT"ITEM # TO CHANGE";T
930 IF T=0 THEN880
940 INPUT"ENTER CORRECT DATA";T(T),Y(T)
950 GOTO840
960 PRINT"DO YOU WANT TO WRITE DATA TO A FILE? (Y OR N)"
970 INPUT R$
980 IF R$<>"Y" THEN 1050
1000 OPEN15,8,15
1010 OPEN5,8,5"@0:"+F$+",S,W"
1020 FOR I=1 TO N
1030 PRINT#5,Y(I)
1040 NEXT I:CLOSE5:CLOSE15
1050 RETURN
```

REFERENCES

1. Mantell, C. L., Adsorption, McGraw-Hill, New York (1945).

2. Hassler, J. W., Purification with Activated Carbon: Industrial Commercial, Environmental, 3rd ed., Chemical Publishing Co., New York (1974).

3. Roberts, P. V., and Summers, R. S., "Performance of Granular Activated Carbon for Total Organic Carbon Removal", Journal AWWA, 74, 113-118 (1982).

4. Adamson, A. T., Physical Chemistry of Surfaces, 4th ed., John Wiley and Sons, New York (1982).

5. Perry, R. H., and Chilton, C. H., editors, Chemical Engineers Handbook, 5th ed., McGraw-Hill, New York (1973).

6. Nguyen, Q. X., "Finite Compartment Model for Design of Carbon Adsorbers for Water and Waste Water", M.S. Thesis, Vanderbilt University (1981).

7. Bohart, G. S., and Adams, E. Q., "Some Aspects of the Behavior of Charcoal with Respect to Chlorine", Journal ACS, 42, 523 (1920).

8. Dole, M., and Klotz, I. M., "Sorption of Chloropicrin and Phosgene on Charcoal from a Flowing Gas Stream", IEC, 38, 11, 1289 (1946).

9. Hutchins, R. A., "Activated Carbon Systems", Chem. Eng., August 20 (1973).

10. Kodavasal, A. S., "Agitated-Batch and Packed Column Activated Carbon Adsorption," Ph.D. Thesis, Vanderbilt University (1978).

11. Suzuki, M. and Smith, J. M., "Axial Dispersion in Beds of Small Particles", Chem. Eng. Jour., 3, 256 (1972).

12. Geankoplis, C. J., and Wilson, E. J., "Liquid Mass Transfer at Very Low Reynolds Numbers in Packed Beds", IEC Fund., 5, 1, 9 (1966).

13. Raceke, K. H., Ortleb, H. J., and Gelbin, D., "Evaluating Breakthrough Curves with Method of Moments for Systems Obeying the Langmuir Isotherm", Chem. Eng. Sci., 36, 11-16 (1981).

14. Michaels, A. S., "Simplified Method of Interpreting Kinetic Data in Fixed Bed Ion Exchange", IEC, 44, 8, 1922 (1952).

15. Treybal, R. E., Mass-Transfer Operations, 3rd ed., McGraw-Hill, New York (1980).

16. Levenspiel, O., Chemical Reactor Engineering, 2nd ed., John Wiley and Sons, New York (1972).

17. Levenspiel, O., The Chemical Reactor Omnibook, Oregon State University, Corvallis, Oregon (1979).

18. Jenson, V. G., and Jeffreys, J. V., Mathematical Methods in Chemical Engineering, 2nd ed., Academic Press, New York (1977).

19. Selby, S. M., editor, Standard Mathematical Tables, 19th ed., The Chemical Rubber Co., Cleveland, Ohio (1971).

20. Haynes, H. W., and Sarma, P. N., "A Model for the Application of Gas Chromatography to Measurements of Diffusion in Bidisperse Structural Catalysts", Department of Chemical Engineering, University of Mississippi.

21. Debelak, K. A., Roth, J. A., and Garrison, D. B., "A Simple Finite Compartment Model for Carbon Adsorbers", AIChE Annual Meeting (1983).

22. Rosene, M. R., et al., "High-Pressure Technique for Rapid Screening of Activated Carbons for Use in Potable Water", in Activated Carbon Adsorption of Organics from the Aqueous Phase, Vol. 1, Suffett, I. H., and McGuire, M. J., editors, Ann Arbor Science, Ann Arbor, Michigan (1980).

23. Liu, Kuang-tsan, "Determination of Mass Transport Parameters for Fixed-Bed Adsorbers by a Microcolumn Technique", Ph.D. Thesis, University of Michigan (1980).

24. Weber, J. W., et al., "Potential Mechanisms for Removal of Humic Acids from Water by Activated Carbon" in Activated Carbon Adsorption of Organics from the Aqueous Phase, Vol. 1, Suffet, I. H., and McGuire, M. J., editors, Ann Arbor Science, Ann Arbor, Michigan (1980).

25. Dean, J. F., editor, Lange's Handbook of Chemistry, 12th ed., McGraw-Hill, New York (1979).

26. Mansour, A. R., "Numerical Solution of Liquid Phase Multicomponent Adsorption in Fixed Beds", Ph.D. Thesis, University of Tulsa (1980).

27. Mansour, A. R., von Rosenberg, D. U., and Sylvester, N. D., "Numerical Solution of Liquid-Phase Multicomponent Adsorption in Fixed Beds", AIChE Journal, 28, 5, 765-771 (1982).

28. Gardener, R. P., and Roges, R. S. C., "Use of a Finite-Stage Transport Concept for Analyzing Residence Time Distributions of Continuous Processes," AIChE Journal, 25, 229 (1979).

29. Weber, W. J., and Crittendon, J. C., "MADAM I-A Numeric Method of Design of Adsorption Systems", Journal WPCF, 47, 5, 924 (1975).

30. Liapis, A. I., and Rippin, D. W. T., "The Simulation of Binary Adsorption in Activated Carbon Columns Using Estimates of Diffusional Resistance within the Carbon Particles Derived from Batch Experiments", Chem. Eng. Sci., 33, 593-600 (1978).

31. Weber, W. J., and Pirbazari, M., "Adsorption of Toxic and Carcinogenic Compounds from Water", Journal AWWA, 74, 203-209 (1982).

END

FILMED

DTIC